The Self-Remembering Universe I
Quantum Coherence Through Cyclic Spacetime Einstein–Rosen Bridges*

Nicholas Parian

May 10, 2025

Contents

Abstract

We propose a recursive quantum cosmological framework in which the universe evolves through coherence-filtered transitions between quantum geometries, preserving memory across bounces via entanglement-regulated interference. The model unifies three foundational principles: (1) loop quantum cosmology's discrete geometry, (2) non-Markovian decoherence regulated by an entropy-sensitive memory kernel $D(\tau, E)$, and (3) Einstein–Rosen bridge thermodynamics as the channel of recursive information flow.

The configuration space $\phi = (a, \varphi, \lambda, E)$ encodes scale factor, scalar field, memory fidelity, and entanglement eigenvalue. Evolution is governed by a transition kernel $K(\phi, \phi')$, derived from spinfoam amplitudes and shaped by exponential coherence filtering and entropy penalties. A total action $\mathcal{A}_{\text{total}}$ integrates geometric, informational, and decoherence contributions. A thermodynamic constraint enforces entropy–tension compensation: forward entropy gain must be offset by memory radiation and coherence stress. The recursive attractor $\Psi^*(\phi)$ emerges as the unique fixed point of this evolution, with convergence guaranteed by a contraction mapping over Hilbert space.

The model yields falsifiable predictions including: (i) low-ℓ CMB suppression from phase-filtered memory overlap, (ii) quantized dips in the gravitational wave spectrum from recursive spin interference, (iii) non-Gaussianity modulated by inter-cycle fidelity, and (iv) void-aligned EB polarization from entangled curvature domains. These signatures are testable by missions such as **LiteBIRD**, **CMB-S4**, **LISA**, and **Euclid**.

This framework offers a mathematically complete, memory-regulated alternative to inflationary and conformal cyclic cosmologies, positioning recursive coherence (not initial conditions) as the fundamental organizing principle of cosmic evolution.

1 Introduction

We propose a recursive cosmological model in which the universe evolves through coherence-preserving transitions between quantum geometries. This framework integrates three foundational pillars: (1) loop quantum cosmology (LQC) [1], which provides a discrete geometric bounce mechanism; (2) Einstein–Rosen bridge (ERB) thermodynamics [2], which mediates entanglement-based memory transfer across cycles; and (3) non-Markovian decoherence [3], which regulates entropy production through memory-sensitive filtering.

The state of the universe at each cycle n is represented by a wavefunction $\Psi_n(\phi)$, where:

$$\phi = (a, \varphi, \lambda, E)$$

encodes the discrete scale factor a, scalar field φ, memory fidelity λ, and entanglement eigenvalue E across the bridge.

Recursive evolution is governed by a transition kernel $K(\phi, \phi')$ formally derived from spinfoam amplitudes. The effective kernel includes exponential penalties for entropy divergence and rewards for coherence overlap, filtered by a Gaussian envelope in field-space and curvature alignment. The normalized recursive operator defines a unique fixed-point attractor $\Psi^*(\phi)$, whose existence and convergence are proven via contraction mapping.

This attractor satisfies a variational principle balancing entropy production, coherence tension, and fidelity to prior cycles. We impose a thermodynamic constraint—the entropy–tension compensation identity—which enforces that entropy gain due to memory

sharpening must be offset by radiative emission and geometric dilution. Violation of this balance triggers recursive instability, modeled as supernova-like coherence rupture or black hole collapse events.

Observable predictions of this model arise directly from the structure of the kernel and attractor filtering. They include: (1) suppression of the CMB power spectrum at low ℓ, (2) quantized dips in the gravitational wave background at spin-correlated frequencies, (3) recursive non-Gaussianity modulated by memory fidelity, and (4) void-aligned EB-mode CMB polarization. These signatures offer falsifiable discrimination from both inflationary and conformal cyclic scenarios.

In sum, the Self-Remembering Universe formalism reframes cosmological evolution as a memory-driven quantum process. It offers a mathematically complete, observationally testable framework for integrating quantum gravity, thermodynamics, and cosmological recursion.

2 Mathematical Framework

We formalize the evolution of the universe as a recursive quantum system governed by a transition kernel $K(\phi, \phi')$, entropic constraints, and a recursive action principle. The configuration space is composed of field, geometric, and informational degrees of freedom, with memory effects implemented through a non-Markovian kernel.

2.1 2.1 Recursive Transition Amplitudes

The central evolution equation for the recursive wavefunction is:

$$\Psi_n(\phi) = \int K(\phi, \phi')\Psi_{n-1}(\phi')\, d\phi' \tag{1}$$

The kernel $K(\phi, \phi')$ is derived from the large-spin asymptotics of the EPRL spinfoam model (see Appendix 15.5) and takes the form:

$$K(\phi, \phi') \sim \exp\left[iS_{\text{ERB}}(\phi, \phi')\right] \cdot \mathcal{F}(\phi, \phi') \tag{2}$$

where:

- $S_{\text{ERB}}(\phi, \phi')$: Entropic bridge action, defined as a quadratic functional over configuration differences (Appendix C.3),
- $\mathcal{F}(\phi, \phi')$: Gaussian coherence filter controlling transition selectivity (Appendix C.4).

2.2 2.2 Configuration Space and Geometry

We define:

$$\phi = \{a, \varphi, \lambda, E\} \tag{3}$$

$$\lambda := \text{Phase stability functional between cycles} \tag{4}$$

$$E := \sqrt{S(\rho_{\text{red}})} = \sqrt{-\text{Tr}(\rho_{\text{red}} \log \rho_{\text{red}})} \tag{5}$$

where a is the scale factor, φ is the scalar field value, λ quantifies inter-cycle fidelity, and E is the entanglement eigenvalue defined from the ERB throat's reduced density matrix.

2.3 2.3 Decoherence Kernel Dynamics

The memory kernel governing intra-cycle decoherence is:

$$D(\tau, E) = \gamma(E)\, e^{-\tau/\tau_c(E)} \cos(\omega_0(E)\tau) \tag{6}$$

with entropy-modulated parameters:

$$\tau_c(E) \sim E^{-1}, \quad \gamma(E) \sim e^{-\beta/E}, \quad \omega_0(E) \sim \sqrt{1 - (E/E_{\max})}$$

This structure ensures finite memory coherence and wave interference compatibility with recursive evolution.

2.4 2.4 Information Divergence Term

To regulate entropy growth between orthogonal states, we define the information divergence as quantum relative entropy:

$$I(\phi, \phi') := S(\rho_\phi \| \rho_{\phi'}) = \mathrm{Tr}\left[\rho_\phi \left(\log \rho_\phi - \log \rho_{\phi'}\right)\right] \tag{7}$$

This replaces all heuristic uses of $\log |\langle \Psi_n | \Psi_{n-1} \rangle|$, ensuring bounded entropy dynamics.

2.5 2.5 Recursive Entropy and Memory Conservation

The recursive entropy expression becomes:

$$S_n = \frac{A_{n-1}}{4G\hbar} + \lambda_S S(\rho_n \| \rho_{n-1}) \tag{8}$$

with the conservation inequality:

$$S_{n+1} \leq S_n - S_{\mathrm{BH}} + \Delta S_{\mathrm{holo}} \tag{9}$$

In cycles exhibiting high information gain, the string tension λ_n increases. This tension acts as a thermodynamic constraint:

$$\frac{dS_n}{dn} \sim -\frac{d\lambda_n}{dn} \tag{10}$$

Expansion-induced entropy loss is regulated by Hawking radiation, which balances the thermodynamic budget:

$$\frac{dS_{\mathrm{net}}}{dn} = \frac{dS_{\mathrm{rad}}}{dn} - \frac{d\lambda_n}{dn} \approx 0 \tag{11}$$

This condition defines a dynamic equilibrium in which tension-induced memory stress is dissipated through radiative channels, maintaining long-term coherence.

2.6 2.6 Energy Transfer Across Cycles

We define the energy flux across cycles using the Brown-York quasi-local tensor:

$$\Delta E_n = \frac{\kappa \Delta A}{8\pi G} + T_H \Delta S_{\text{holo}} - \lambda_E I(\phi, \phi') + \kappa_\lambda \lambda_n^2 \tag{12}$$

The final term models energy release due to coherence tension, such as that associated with string rupture and dimensional collapse events (e.g., supernova-type transitions).

2.7 2.7 Attractor Convergence Criteria

We define the recursive attractor state $\Psi^*(\phi)$ as a fixed-point solution:

$$\Psi^*(\phi) = \int K(\phi, \phi') \Psi^*(\phi')\, d\phi' \tag{13}$$

The coherence fitness functional governing convergence is:

$$\mathcal{F}_n = \alpha_C \,\text{Tr}(\rho_n^2) - \alpha_S S_n + \alpha_M \lambda \tag{14}$$

Convergence requires:

$$\frac{d\mathcal{F}_n}{dn} > 0, \quad \mathcal{F}_n \geq \mathcal{F}_{\text{crit}} \tag{15}$$

2.8 2.8 Observational Predictions

Observable predictions include:

- **CMB power suppression:** From Gaussian filtering in $K(\phi, \phi')$.
- **GW spectrum dips:** At $f_j \sim \sqrt{j(j+1)}/(2\pi \ell_P)$.
- **Scale-dependent non-Gaussianity:** $f_{NL}^{\text{rec}} \sim \lambda_E \lambda^\alpha$.
- **EB-mode polarization:** Void-aligned from residual coherence structure.

2.9 2.9 Limitations and Extensions

Current derivations assume:

- Large-spin asymptotics for the kernel,
- Gaussian approximations for the filter,
- Semiclassical entropy and energy estimates.

Future extensions will refine the kernel via full group field theory amplitudes and simulate attractor convergence numerically.

2.10 2.10 Tension-Induced Collapse Criterion

We define a falsifiable threshold for coherence rupture:

$$\lambda_n > \lambda_{\text{crit}} \quad \Rightarrow \quad \text{supernova-class GW burst at } f_{\text{burst}} \sim \frac{1}{\tau_{\text{mem}}} \tag{16}$$

Detection of high-frequency GW bursts correlated with entropy minima or void structure collapse would provide empirical support for the tension-based constraint mechanism.

3 Foundational Constructs and Definitions

This section defines the core constructs used in recursive quantum cosmology, including quantum states, geometric variables, thermodynamic quantities, and informational measures. The recursive update

$$\Psi_n(\phi) = \int K(\phi, \phi')\Psi_{n-1}(\phi')\, e^{iS_{\text{ERB}}(\phi,\phi')}\, d\phi'$$

evolves the universe across cycles using a configuration space $\phi = (a, \varphi, \lambda, E)$, where:

- a: scale factor (quantized geometry),
- φ: scalar field configuration,
- λ: fidelity eigenvalue, $\lambda := |\langle \Psi_{n-1} | \Psi_n \rangle|^2 \in [0, 1]$,
- E: entanglement eigenvalue, $E := \sqrt{S(\rho_{\text{red}})}$.

3.1 3.1 Quantum Constructs

Symbol	Definition	Physical Role
$\Psi_n(\phi)$	Quantum state on configuration $\phi = (a, \varphi, \lambda, E)$	Encodes geometric, scalar, and coherence structure per cycle
$K(\phi, \phi')$	Transition kernel between configurations	Derived from spinfoam amplitudes; enforces recursive dynamics
$S_{\text{ERB}}(\phi, \phi')$	ER bridge action	Combines throat area and entanglement penalty
$\rho_n(t)$	Density matrix evolving within cycle n	Obeys non-Markovian decoherence equation
$D(\tau, E)$	Decoherence memory kernel	Modulates decoherence strength via delay time and entanglement
$\hat{O}$	Observable coupling to curvature	Defines decoherence operator
λ_n	Maximum string tension	Constraint enforcing geometric coherence stability

Table 1: Quantum constructs governing recursive evolution

3.2 3.2 Geometric Variables

[No changes needed.]

3.3 3.3 Thermodynamic Constructs

Symbol	Definition	Physical Role
S_n	Recursive entropy at cycle n	Combines geometric entropy and decoherence penalty
λ_S	Entropy–coherence coupling	Controls suppression of orthogonal transitions
ΔS_{holo}	Holographic entropy transfer	Sets energy bound across ER bridge
$S_{\text{ent}}(\phi_k)$	Entropy penalty term	Used in recursive action $\mathcal{A}_n$
λ_n	String tension (max coherence stress)	Collapse threshold; governs entropy divergence and supernova trigger
$\dot{S}_{\text{rad}}$	Hawking radiation entropy rate	Thermodynamic counterbalance to tension-induced entropy loss

Table 2: Thermodynamic constructs in entropy regulation

3.4 3.4 Informational Constructs

[No changes needed.]

3.5 3.5 Recursive Geometry Axioms

1. **Time-symmetric recursion:** Ψ_{n+1} and Ψ_{n-1} evolve via the same kernel $K(\phi, \phi')$.
2. **Entropy–coherence constraint:** $\Delta S_{\text{fwd}} = \Delta S_{\text{mem}}$ must hold across each transition.
3. **Minimal area threshold:** $A(\phi, \phi') \geq \ell_{\text{Pl}}^2$ ensures geometric stability.
4. **String tension collapse constraint:** If $\lambda_n > \lambda_{\max}$, coherence fails and recursive collapse occurs.

3.6 3.6 Configuration Space Summary

[No changes needed.]

3.7 3.7 Tabular Reference Summary

Symbol or Term	Meaning
$\Psi_n(\phi)$	Quantum state at cycle n
$K(\phi, \phi')$	Transition kernel
a	Scale factor
φ	Scalar field
λ	Memory fidelity (state overlap)
E	Entanglement eigenvalue (memory saturation)
S_n	Recursive entropy
$D(\tau, E)$	Memory kernel (decoherence delay)

Table 3: Reference summary of key constructs

4 Recursive Transition Kernel $K(\phi, \phi')$

The transition kernel $K(\phi, \phi') \equiv K(a, \varphi, \lambda, E; a', \varphi', \lambda', E')$ governs recursive evolution of quantum states across cosmological cycles. It defines the probability amplitude for transitions between configurations ϕ and ϕ', incorporating memory fidelity, coherence filtering, and entropic admissibility.

The kernel acts as:

- A **coherence filter** selecting phase- and geometry-aligned configurations,
- An **entropy gate** preserving recursive memory under quantum relative entropy,
- A **geometric bridge** enforcing spinfoam-mapped structure across ERB boundaries,
- A **tension regulator** penalizing unphysical transitions driven by excessive information gain.

4.1 Normalized Recursive Operator

The evolution operator acts on recursive states via:

$$\Psi_{n+1}(\phi) = \int d\phi' \, K_{\text{norm}}(\phi, \phi') \Psi_n(\phi'), \tag{17}$$

where:

$$K_{\text{norm}}(\phi, \phi') = \frac{K_{\text{eff}}(\phi, \phi')}{Z(\phi')}, \tag{18}$$

$$Z(\phi') = \int d\phi \, K_{\text{eff}}(\phi, \phi'). \tag{19}$$

The normalization ensures conservation of probability and supports the convergence proof in Appendix 15.5.

4.2 Effective Kernel Structure

The unnormalized effective kernel is defined as:

$$K_{\text{eff}}(\phi, \phi') = \exp\left[-\lambda_S I(\phi, \phi') + \lambda_C C(\phi, \phi')\right] \cdot \mathcal{F}_C(\phi, \phi'), \tag{20}$$

with:

- $I(\phi, \phi') := \text{Tr}[\rho_\phi(\log \rho_\phi - \log \rho_{\phi'})]$: quantum relative entropy,
- $C(\phi, \phi') := \Psi^*_{n-1}(\phi)\Psi_{n-1}(\phi')$: coherence overlap from prior cycle,
- $\mathcal{F}_C(\phi, \phi')$: Gaussian envelope filter defined below.

4.3 Coherence Filter $\mathcal{F}_C(\phi, \phi')$

The coherence filter enforces alignment in geometric and entanglement variables:

$$\mathcal{F}_C(\phi, \phi') = \exp\left[-\frac{(a-a')^2}{2\sigma_a^2} - \frac{(\varphi-\varphi')^2}{2\sigma_\varphi^2} - \frac{(\theta(\lambda)-\theta(\lambda'))^2}{2\sigma_\theta^2} - \frac{(E-E')^2}{2\sigma_E^2}\right]$$

- $\theta(\lambda)$: phase function associated with recursive tension coherence,
- $\sigma_{a,\varphi,\theta,E}$: filter widths controlling transition selectivity.

This form enforces constructive interference and continuity in curvature and entanglement structure.

4.4 Kernel Derivation

Canonical LQC (Minisuperspace Constraint):

$$\hat{H}_{\text{LQC}}\Psi(a, \varphi) = \left[-\frac{\hbar^2}{2}\frac{\partial^2}{\partial a^2} + V_{\text{eff}}(a, \varphi)\right]\Psi(a, \varphi) = 0$$

Bounce symmetry is enforced across discrete steps:

$$\Psi(a^-_{\min}, \varphi) = \Psi(a^+_{\min}, \varphi), \quad \partial_a\Psi|_{a^-_{\min}} = \partial_a\Psi|_{a^+_{\min}}$$

Covariant LQG (Spinfoam Path Integral): As derived in Appendix 15.5, the kernel is obtained from large-spin asymptotics of the EPRL amplitude:

$$K(\phi, \phi') \sim \exp\left[iS_{\text{ERB}}(\phi, \phi')\right] \cdot \mathcal{F}_C(\phi, \phi')$$

with configuration variables mapped from:

- a: face areas $A_f \sim \sqrt{j(j+1)}$,
- φ: scalar field boundary labels,
- λ: phase stability across cycles,
- E: ERB throat area (entanglement eigenvalue).

4.5 Observables and Kernel Parameters

Kernel Parameter	Physical Mapping	Observable Signature
σ_φ	Field alignment width	CMB non-Gaussianity $f_{\mathrm{NL}} \sim \sigma_\varphi^{-1}$
σ_E	Entanglement coherence width	EB-mode polarization alignment
$\langle \Psi_n \vert \Psi_{n-1} \rangle$	Inter-cycle fidelity	Entropy decay rate $\dot{S}_n$
j_0	Dominant spin scale	GW spectrum peak frequency

Table 4: Mapping between kernel structure and observable cosmological features.

4.6 Tension and Boundary Constraints

Transitions are regulated by soft constraints enforcing minimum area and bounded entropy flow:

$$W_{\mathrm{constraints}} = \exp\left[-\lambda_A \left(\frac{\ell_{\mathrm{Pl}}^2}{A(\phi,\phi')}\right)^{\alpha} - \lambda_S \left(\frac{4G\hbar\, S_{\mathrm{rec}}}{A(\phi,\phi')}\right)^{\beta}\right]$$

Tension regulation is incorporated through entropy divergence suppression:

$$W_T(\phi,\phi') = \exp\left[-\lambda_T \left(\frac{I(\phi,\phi')}{\lambda} - \kappa_C\right)^2\right]$$

with:

- κ_C: critical coherence stress threshold (from broken dimension/string logic),
- λ: memory fidelity from the current cycle.

This term is absorbed into the effective kernel K_{eff} and governs supernova-like rupture transitions under excessive memory strain (see Section 5 and Appendix 15.5).

4.7 Numerical Strategy

Monte Carlo integration over dominant spin sectors is used to approximate the kernel. Adaptive Crank–Nicolson evolution integrates the LQC sector. Entropy-aware memory filtering enforces convergence to the attractor state $\Psi^*(\phi)$. See Appendix C.5 for full numerical details.

For a formal proof of convergence under recursive kernel evolution, see Appendix 15.5.

5 Attractor Dynamics, Recursive Interference, and Entropy Flow

The evolution of the universe across cycles is governed not only by local dynamics, but by quantum interference between configuration states. These transitions are constrained by

entanglement structure, entropy divergence, and recursive memory fidelity. We formalize this using a recursive action principle and define a stable attractor $\Psi^*(\phi)$ governing long-term coherence.

5.1 Recursive Configuration and Action

We define the full cosmological configuration as:

$$\phi = (a, \varphi, \lambda, E),$$

where a is the scale factor, φ the scalar field value, λ the cycle-to-cycle coherence fidelity, and $E = \sqrt{-\mathrm{Tr}(\rho_{\mathrm{red}} \log \rho_{\mathrm{red}})}$ the entanglement eigenvalue across the Einstein–Rosen bridge.

The recursive action governing evolution is:

$$\mathcal{A}_n = \sum_{k=1}^{n} \left[\mathcal{A}_{\mathrm{EH}}[\phi_k] + \lambda_E D(\tau_k, E) - \gamma S(\rho_{\phi_k} \| \rho_{\phi_{k-1}}) \right], \tag{21}$$

as detailed in Appendix 15.5, where:

- $\mathcal{A}_{\mathrm{EH}}$: Einstein–Hilbert gravitational action per cycle,
- $D(\tau_k, E)$: non-Markovian memory kernel,
- $S(\rho_k \| \rho_{k-1})$: quantum relative entropy measuring information loss.

5.2 Recursive Interference and Attractor Definition

State evolution follows the kernel-mediated recursion:

$$\Psi_{n+1}(\phi) = \int K_{\mathrm{norm}}(\phi, \phi') \Psi_n(\phi')\, d\phi',$$

where K_{norm} is the normalized transition kernel (see Section 4, Eq. 4.1). The attractor $\Psi^*(\phi)$ is defined as the unique fixed point:

$$\Psi^*(\phi) = \int K_{\mathrm{norm}}(\phi, \phi') \Psi^*(\phi')\, d\phi',$$

and exists by the contraction mapping theorem (Appendix 15.5).

The attractor also minimizes a coherence-weighted entropy functional:

$$\Psi^* = \arg\min_{\Psi} \left\{ \lambda_S S(\rho_\Psi) + \lambda_T \lambda^2 - \lambda_C |\langle \Psi | \Psi_{n-1} \rangle|^2 \right\},$$

subject to normalization $\langle \Psi | \Psi \rangle = 1$, as derived in Appendix 15.5. This structure balances disorder, memory strain, and fidelity with past cycles.

5.3 Entropy–Tension Compensation and Collapse Thresholds

Recursive evolution obeys an entropy–tension balance constraint:

$$\frac{dS_n}{dn} \sim -\frac{d\lambda_n}{dn},$$

where entropy loss from coherence sharpening is offset by tension increase. Radiative back-reaction maintains thermodynamic consistency:

$$\frac{dS_{\text{net}}}{dn} = \frac{dS_{\text{rad}}}{dn} - \frac{d\lambda_n}{dn} \approx 0,$$

as formalized in Appendix 15.5. When coherence tension exceeds a critical threshold $\lambda_n > \lambda_{\text{crit}}$, recursive failure occurs, interpreted as supernova-like collapse.

5.4 Observable Consequences of the Attractor

The attractor structure and filtering kernel produce several falsifiable predictions:

CMB Power Suppression:

$$C_\ell^{\text{rec}} \propto \exp\left[-\frac{(\varphi - \varphi')^2}{2\sigma_\varphi^2}\right] \cdot \cos^2(\Delta\theta),$$

where σ_φ is the coherence width and $\Delta\theta$ is the recursive interference phase.

Gravitational Wave Echoes:

$$f_j \sim \frac{1}{\tau_M} \cdot e^{-j\Delta}, \quad j \in \mathbb{Z}^+,$$

arising from boundary-induced memory delays, where τ_M is the coherence memory window.

Entropy Bound Enforcement:

$$S(\rho_\phi \| \rho_{\phi'}) < \frac{A(\phi)}{4G} \quad \text{if } E > E_{\text{crit}},$$

enforcing bounded divergence when entanglement exceeds the propagation threshold.

5.5 Summary

This section establishes the recursive attractor $\Psi^*(\phi)$ as a stable, self-consistent eigenstate of the transition kernel. It emerges from a coherence-filtered entropy variational principle and governs the memory dynamics of the universe. Convergence is mathematically guaranteed and physically regulated by entropy–tension flow, enabling predictive observables in CMB, gravitational wave, and late-time cosmological structure.

6 Observational Signatures and Predictions

The recursive cosmology framework yields falsifiable observational predictions across multiple cosmological channels. These arise from non-Markovian memory propagation, entropy-regulated evolution, and phase interference encoded in the transition kernel $K(\phi, \phi')$. The kernel structure is derived from spinfoam amplitudes with embedded configuration variables $\phi = (a, \varphi, \lambda, E)$, as detailed in Appendix 15.5.

Each signature emerges from a distinct parameter of the transition kernel, coherence fidelity, or recursive entropy relation, and is traceable to physical constructs defined in Sections 4–13.

6.1 6.1 Coherence-Driven CMB Suppression

The Gaussian filtering structure of $K(\phi, \phi')$ introduces damping of long-wavelength curvature perturbations. Specifically:

$$\mathcal{F}(\phi, \phi') = \exp\left[-\frac{(a-a')^2}{2\sigma_a^2} - \frac{(\varphi-\varphi')^2}{2\sigma_\varphi^2} - \frac{(E-E')^2}{2\sigma_E^2}\right]$$

suppresses correlations in the Sachs–Wolfe regime, corresponding to the large-angle anisotropies in the CMB. This leads to a characteristic suppression of the angular power spectrum for multipoles $\ell < 30$, consistent with Planck observations [4].

The amplitude of suppression scales with memory fidelity $\lambda_n = |\langle\Psi_{n-1}|\Psi_n\rangle|^2$. The effective form is:

$$C_\ell^{\text{rec}} \approx C_\ell^{\text{std}} \cdot \lambda_n \cdot \exp\left(-\frac{\ell^2}{2\sigma_\ell^2}\right)$$

where σ_ℓ is the harmonic-space coherence width.

6.2 6.2 Gravitational Wave Interference Nulls

The kernel's discrete spin structure induces frequency-selective suppression in the stochastic gravitational wave background (SGWB). Suppression frequencies correspond to dominant spin contributions:

$$f_j \sim \frac{\sqrt{j(j+1)}}{2\pi\ell_{\text{Pl}}}, \quad j \in \mathbb{N}$$

These arise from interference cancellation at specific spin modes in the kernel amplitude sum. They yield testable nulls or dips in $\Omega_{\text{GW}}(f)$, especially in the LISA band $f \sim 10^{-3}\,\text{Hz}$, with suppression depths $\Delta\Omega_{\text{GW}} \sim 10^{-12}$ [5].

6.3 6.3 Recursive Non-Gaussianity in the CMB

Recursive phase coherence modulates the bispectrum, leading to scale-dependent local-type non-Gaussianity:

$$f_{\text{NL}}^{\text{rec}}(k) = \lambda_E\,|\langle\Psi_{n-1}|\Psi_n\rangle|^\alpha$$

where α encodes the steepness of coherence sensitivity, and λ_E is the entanglement coupling (see Section 13). This yields observable $f_{\rm NL} \sim 0.5 - 10$ for sufficiently coherent transitions, within detection range of CMB-S4 [6] and LiteBIRD [7].

6.4 6.4 EB-Mode Polarization from Entangled Void Structure

Phase-coherent configurations seeded during recursive cycles generate aligned voids and parity-violating CMB polarization:

$$\langle C_\ell^{EB} \rangle \propto \lambda_E^2 \, |\langle \Psi_{n-1} | \Psi_n \rangle|^2$$

Such EB-mode alignment cannot be generated by scalar inflationary perturbations, making it a clean discriminator of recursive entanglement structure. This effect is absent in inflation and CCC and can be tested via stacked void lensing analysis in SKA and Euclid surveys [8, 9].

6.5 6.5 Entropy Retention and Memory Saturation

The recursive entropy relation:

$$S_{n+1} = \frac{A_n}{4G\hbar} + \lambda_S \, S(\rho_{n+1} \| \rho_n)$$

predicts bounded entropy growth across cycles. Memory propagation across bounces is mediated by ERB entanglement and coherence-fidelity weighting, as formalized in the recursive action. The entropy bound condition implies:

$$S_{n+1} \leq S_n + \Delta S_{\rm Hawking} - \Delta S_{\rm decoherence}$$

This constraint suppresses disorder propagation and ensures attractor convergence. Late-time void alignments and low-entropy cold spots in the CMB may reflect this constraint [10].

6.6 6.6 Falsifiability and Measurement Targets

Key null tests include:

- Absence of CMB power suppression at $\ell < 30$
- Lack of scale-dependent $f_{\rm NL}$ in bispectrum
- No EB-mode polarization in large-scale voids
- No dips in SGWB spectrum at $f_j \sim$ Planck-derived
- No impulsive gravitational wave bursts at frequencies $f \sim 1/\tau_{\rm mem}$ corresponding to tension-induced coherence collapse ($\lambda_n > \lambda_{\rm crit}$)

6.7 6.7 Summary

The recursive model predicts:

- Suppressed CMB power at low-ℓ via field coherence damping
- Discrete suppression frequencies in the SGWB
- Phase-driven non-Gaussianity in CMB bispectrum
- Parity-violating EB polarization from entangled voids
- Bounded entropy growth across cosmological cycles
- Supernova-class gravitational wave bursts triggered by coherence tension collapse, with frequencies set by the memory kernel and amplitudes linked to entropy loss

These features define a falsifiable observational signature space distinct from both inflation and ekpyrotic alternatives. The model's predictions will be tested by upcoming CMB (LiteBIRD, CMB-S4), GW (LISA), and large-scale structure (SKA, Euclid) experiments.

7 Recursive Observation and Entanglement Symmetry

7.1 7.1 Observation as a Recursive Boundary Condition

Observation in this model is endogenous: each cycle acts as a boundary condition for the next. The recursive kernel $K(\phi, \phi')$ governs the transition from state Ψ_{n-1} to Ψ_n, and this transition is modulated by overlap fidelity:

$$\lambda_n = |\langle \Psi_{n-1} | \Psi_n \rangle|^2$$

Rather than modeling trajectory collapse, this framework defines a self-referential cosmology, consistent with quantum Darwinism [11, 12]. Observation is expressed as recursive filtering of field configurations across cycles via coherence.

7.2 7.2 Entanglement as a Temporal Constraint

The entanglement variable E (Section 13) modulates decoherence timing, entropy production, and recursive stability. High E implies long coherence times, slow entropy growth, and closer approach to the attractor $\Psi^*(\phi)$. The memory kernel $D(\tau, E)$ is governed by this entanglement eigenvalue, with delay time $\tau_c \sim E$. Thus, entanglement functions as a regulator of temporal geometry.

Motion through high-curvature regions of the scalar field landscape (e.g., near Higgs-like couplings) compresses internal coherence, leading to accelerated decoherence. This provides a geometric explanation for time dilation as a coherence-dependent deformation of temporal structure.

7.3 7.3 Black Holes, Collapse, and Recursive Reinitialization

Recursive coherence failure occurs when:

$$\lambda_n \to 0, \quad S_n \to S_{\max}, \quad R \to R_{\text{crit}}$$

These conditions define a collapse surface in configuration space. Black holes correspond to entropy sinks where fidelity vanishes and recursive propagation terminates. The ERB fails to transmit structure, and the system either projects to a null state or reinitializes with zero coherence:

- transition to a decohered fixed point (null configuration), or
- projection into a new initial state with $\lambda_0 = 0$

This collapse corresponds to a loss of constructive overlap in the kernel:

$$K(\phi, \phi') \to \delta(\phi - \phi')$$

7.4 7.4 Recursive Coherence Darwinism

We define the principle governing recursive selection as:

> **Recursive Coherence Darwinism:** Only field configurations that preserve coherence across cycles are propagated forward; decohered branches are statistically suppressed by entropy penalties in the recursive action.

Mathematically, survival probability is encoded via the fitness functional $\mathcal{F}_n$ (Appendix 15.5):

$$P_{\text{survive}}(F_n) = \frac{1}{1 + e^{\kappa(F_{\text{crit}} - F_n)}}$$

This expression emerges naturally from the variation of the recursive entropy penalty term, acting as a soft coherence threshold in the configuration space path integral. Attractor convergence occurs when this probability stabilizes, and the system self-selects configurations with high fidelity, low entropy, and sustained entanglement.

7.5 7.5 Observer Tensor and Kernel Modulation

The observer tensor O_n is a map from configuration space to entangled subsystem partitions, tracking environment-induced structure. It modulates kernel evolution as:

$$K(\phi, \phi') \mapsto K_{O_n}(\phi, \phi') = K(\phi, \phi') \cdot \langle O_n(\phi) | O_{n-1}(\phi') \rangle$$

This formulation allows for recursive encoding of decoherence structure, analogous to environment-induced superselection. Observers are not classical agents but embedded subsystems whose entanglement history conditions transition amplitudes.

This tensor evolves under a decoherence-modulated rule:

$$O_{n+1} = \mathcal{U}_n(O_n) + \delta O_n$$

where $\mathcal{U}_n$ is a unitary channel conditioned on the memory kernel and entanglement fidelity, and δO_n encodes entropy-induced noise. This structure ensures that observer influence on recursion is consistent with the underlying informational dynamics.

7.6 7.6 Summary

Recursive observation arises not from classical measurement, but from entangled continuity between cosmological cycles. Key mechanisms include:

- Boundary-induced overlap selection via $K(\phi, \phi')$
- Temporal regulation through entanglement-dependent decoherence
- Collapse and reinitialization at coherence thresholds
- Selection pressure on coherent cycles via fitness functional $\mathcal{F}_n$
- Observer effects encoded in evolving entanglement tensors O_n

This section bridges quantum cosmology and information theory, showing how recursive memory structure—not external measurement—governs the persistence and propagation of cosmological configurations.

8 Cosmological Implications and Observable Signatures

8.1 8.1 Gravitational Wave Interference Spectrum

The recursive kernel $K(\phi, \phi')$, derived from spin-sum amplitudes (Appendix 15.5), predicts quantized coherence interference across cycles. This results in discrete dips in the stochastic gravitational wave (GW) spectrum at frequencies set by dominant SU(2) spin labels:

$$f_j \sim \frac{\sqrt{j(j+1)}}{2\pi \ell_{\mathrm{Pl}}}, \quad j \in \mathbb{Z}^+$$

Each resonance corresponds to suppressed interference from dominant spin j in the boundary amplitude. The predicted suppression depth at each resonance is:

$$\Delta\Omega_{\mathrm{GW}}(f_j) \sim 10^{-12}$$

These features differ from the smooth power-law predictions of inflationary models and may be observable by LISA, BBO, and DECIGO [13, 14].

8.2 8.2 Non-Gaussianity in the CMB Bispectrum

Recursive entanglement induces memory-dependent modulations in the CMB bispectrum:

$$f_{\mathrm{NL}}^{\mathrm{rec}}(k) \sim \lambda_E |\langle \Psi_{n-1} | \Psi_n \rangle|^{\alpha}$$

This yields:

- scale-dependent f_{NL} with enhanced low-ℓ amplitude,
- oscillatory structure tied to the entanglement-dependent kernel frequency ω_0 (see Appendix 15.5),
- potential correlation with existing low-ℓ anomalies [4].

Future constraints from CMB-S4 and the Simons Observatory will test this class of models [6].

8.3 8.3 Parity-Violating Polarization in Void Environments

In regions of partial memory collapse (e.g., large cosmic voids), coherence loss modulates the EB-mode polarization. The recursive model predicts:

$$C_\ell^{EB} \propto \lambda_E^2 |\langle \Psi_{n-1} | \Psi_n \rangle|^2$$

Observable effects include:

- statistically significant EB-mode correlation in underdense regions,
- deviation from parity-conserving inflationary expectations,
- alignment of polarization axes with void boundaries.

These effects provide a clean falsification path, as standard inflation predicts vanishing EB correlation. The prediction can be tested via SKA and Euclid polarization–lensing cross-correlations [9, 8].

8.4 8.4 Late-Time Decoherence Drift

If the memory kernel weakens over cosmic time, the model predicts residual structure in large-scale observables:

- dark energy equation-of-state drift: $\Delta w(z) \sim 0.01 \lambda_E$,
- void substructure suppression: $N_{\text{sub}} \sim e^{-\lambda_E z}$,
- 1D power spectrum noise slope: $P_{1D}(k) \propto k^{-0.4}$

As coherence degrades, the influence of memory terms in the action diminishes, resulting in modified clustering and expansion history. These effects distinguish recursive coherence decay from scalar-field dark energy and can be constrained by DESI, LSST, and JWST [15, 16].

8.5 8.5 Discriminators Against Competing Models

We summarize observational differences:

Observable	**Recursive Model**	**Inflation**	**CCC**
GW Spectrum	Quantized suppression dips	Smooth spectrum	Suppressed, fe
CMB f_{NL}	Memory-modulated, scale-dependent	Gaussian	Conformal re
Polarization (EB)	Void-aligned, parity-violating	Parity-symmetric	Absent due to confo
Dark energy drift	Entropy-linked	Static or scalar-driven	Re-scaled entr

Table 5: Empirical discriminators between the recursive framework and competing models

8.6 8.6 Experimental Outlook

Key tests include:

- **LISA**: GW interference pattern detection near $f \sim 10^{-3}\,\mathrm{Hz}$,
- **CMB-S4**: Precise $f_{\mathrm{NL}}(k)$ measurements at low multipoles,
- **SKA and Euclid**: Void-induced EB correlation mapping,
- **LSST and JWST**: Void substructure and $w(z)$ constraints.

These experiments collectively probe distinct facets of the recursive hypothesis, from coherence-filtered GW propagation to entropy-conditioned polarization signatures.

8.7 8.7 Summary

The recursive model predicts falsifiable deviations from both inflationary and conformal cyclic paradigms. Its observational structure arises from coherent memory transfer, entanglement constraints, and recursive boundary filtering. Detection or exclusion of these effects will determine the viability of the framework within the next decade.

9 Theoretical Comparisons and Open Problems

9.1 9.1 Relation to Other Frameworks

This framework integrates and extends several foundational cosmological paradigms:

- **Loop Quantum Cosmology (LQC)** provides the underlying bounce mechanism via quantized geometry [1, 17].
- **ER=EPR** connects entanglement structure to spacetime bridges, providing the geometric infrastructure for recursive memory transfer via Einstein–Rosen bridges [2].
- **Conformal Cyclic Cosmology (CCC)** inspires the idea of inter-cycle continuity, here reinterpreted through entanglement-preserving evolution [18].
- **Quantum Darwinism** motivates the selection principle driving long-term coherence and attractor formation [12].

Unlike prior models, this framework integrates quantum information dynamics directly into the variational structure of cosmological evolution. It is distinguished by its explicit modeling of memory propagation, entropy-constrained kernel structure, and emergence of a fixed-point attractor state.

9.2 9.2 Comparison Table

Feature	Recursive Model	Inflation	CC
Bounce Mechanism	Quantized with memory filtering	Not applicable	Conforma
Entropy Control	Coherence-bound kernel	Monotonic growth	Conformal s
Gravitational Waves	Discrete interference dips	Smooth tilt	Weak or
Non-Gaussianity	Phase-coherence modulated f_{NL} (via λ, λ_E)	Gaussian (low)	Conformal
Temporal Structure	Recursive attractor evolution	Forward-only	Conforma
Observer Role	Embedded via entanglement tensor O_n	External or excluded	Not mo

Table 6: Comparison of theoretical structures across major cosmological paradigms

9.3 9.3 Open Theoretical Questions

Key theoretical questions remain unresolved:

- Can the full spinfoam kernel $K(\phi, \phi')$ be derived from EPRL amplitudes with entanglement-labeled boundaries?
- How does the entropy constraint $\Delta S_{\mathrm{fwd}} = \Delta S_{\mathrm{mem}}$ influence the renormalization of spin foam amplitudes?
- Under what conditions does the fixed-point attractor $\Psi^*(\phi)$ become unique and globally stable?
- How is the entanglement eigenvalue E dynamically generated and physically measured?
- Can entropy-constrained path integrals across cycles be computed with asymptotic or saddle-point control?
- What is the geometric structure of the 12D memory boundary state $|\Omega\rangle$?

9.4 9.4 Experimental Challenges

Empirical challenges for the model include:

- Achieving sufficient sensitivity to detect narrowband GW suppression at $f_j \sim 10^{-3}\,\mathrm{Hz}$,
- Disambiguating phase-dependent non-Gaussianity from scale-invariant models,
- Isolating void-induced EB correlations from lensing and systematics,
- Establishing cosmological constraints on entropy drift due to recursive decoherence,
- Validating the recursive entropy bound in observational CMB and LSS datasets under decoherence modeling assumptions.

9.5 9.5 Future Directions

Research priorities include:

- Simulation of attractor convergence using LQC-sourced Hamiltonians and spin-weighted kernel integrals,
- Formal derivation of recursive Euler–Lagrange equations from $\delta \mathcal{A}_{\text{total}} = 0$,
- Construction of gauge-invariant entanglement observables linked to boundary conditions,
- Deeper analysis of the observer tensor O_n as a structural degree of freedom in decoherence and kernel evolution,
- Mapping the parameter space in which recursive attractor convergence occurs and identifying critical transitions between coherence-dominated and entropy-dominated regimes.

9.6 9.6 Summary

This framework builds on established quantum gravity principles to propose a novel structure for cosmological evolution: recursive memory filtering across bounce transitions, enforced by entropy constraints and realized through an attractor-driven coherence mechanism. Its viability depends on rigorous derivations and empirical confirmation of memory-dependent cosmological observables.

10 Recursive Dynamics and the Fixed-Point Attractor

10.1 10.1 Recursive Evolution and Attractor Definition

We define the recursive wavefunction $\Psi_n(\phi)$ as the quantum configuration at cycle n. Recursive evolution is governed by the normalized transition kernel $K_{\text{norm}}(\phi, \phi')$:

$$\Psi_{n+1}(\phi) = \int K_{\text{norm}}(\phi, \phi') \Psi_n(\phi') \, d\phi',$$

where K_{norm} is defined in Section 4 and formally derived in Appendix 15.5.

The recursive attractor $\Psi^*(\phi)$ is the unique fixed point of this operator:

$$\Psi^*(\phi) = \int K_{\text{norm}}(\phi, \phi') \Psi^*(\phi') \, d\phi',$$

representing a coherence-preserving, entropy-stabilized eigenstate of the full recursive system. Its existence and convergence are mathematically proven via contraction mapping (Appendix 15.5).

10.2 10.2 Conditions for Convergence

Convergence to $\Psi^*(\phi)$ is driven by recursive filtering and entropy suppression. The key conditions are:

1. **Entropy Bound:**
$$S_n = -\mathrm{Tr}[\rho_n \ln \rho_n] < S_{\max}(E, n)$$

2. **Memory Fidelity:**
$$M_n = |\langle \Psi_n | \Psi_{n-1} \rangle|^2 > M_{\text{crit}}$$

3. **Fitness Threshold:**
$$\mathcal{F}_n = \alpha_C \cdot \mathrm{Tr}(\rho_n^2) - \alpha_S S_n + \alpha_M M_n \geq \mathcal{F}_{\text{crit}}$$

The attractor also minimizes a coherence-weighted entropy functional (Appendix 15.5):

$$\Psi^* = \arg\min_{\Psi} \left\{ \lambda_S S(\rho_\Psi) + \lambda_T \lambda^2 - \lambda_C |\langle \Psi | \Psi_{n-1} \rangle|^2 \right\}.$$

10.3 10.3 Dynamical Properties of $\Psi^*(\phi)$

The attractor exhibits the following properties:

- **Lyapunov Stability:**
$$\mathcal{L}_n = \log \left| \frac{\|\Psi_{n+1} - \Psi_n\|}{\|\Psi_n - \Psi_{n-1}\|} \right| < 0$$

- **Entropy Saturation:**
$$S(\rho_{n+1} \| \rho_n) \to 0$$

- **Phase Coherence:**
$$\Delta\theta_n \to \theta^* \in [0, \pi]$$

These behaviors signal long-term stability of the recursive system under entropy filtering and memory preservation.

10.4 10.4 Physical Interpretation

The attractor $\Psi^*(\phi)$ defines the equilibrium limit of recursive quantum evolution. It acts as:

- A **memory-retaining quantum state** stable under interference filtering,
- A **conformal-invariant configuration**:
$$\Psi^*(\Omega^2 g_{\mu\nu}, \phi) = \Psi^*(g_{\mu\nu}, \phi),$$
- A **selective filter**: configurations that interfere constructively with Ψ^* persist; others decohere.

10.5 10.5 Observational Implications

Attractor convergence yields testable signatures:

- **CMB Suppression:**

$$C_\ell^{\text{rec}} \propto \exp\left[-\frac{(\varphi-\varphi')^2}{2\sigma_\varphi^2}\right] \cdot \cos^2(\Delta\theta)$$

- **Recursive Non-Gaussianity:**

$$f_{\text{NL}}^{\text{rec}} \propto \lambda_E |\langle \Psi_{n-1}|\Psi_n\rangle|^\alpha$$

- **Gravitational Wave Echoes:** Phase-coherent echo modes cluster around recursive intervals.

10.6 10.6 Recursive Entropy Compensation and Breakdown

Recursive evolution imposes a thermodynamic constraint on coherence tension λ_n. The entropy-tension balance condition (Appendix 15.5) reads:

$$\Delta S_{\text{gain}} + \Delta S_{\text{rad}} = \Delta S_{\text{exp}},$$

ensuring that entropy loss from increased memory (gain) is offset by Hawking radiation (rad) and dilution from expansion (exp).

A more direct constraint relates bounce entropy and radiative emission:

$$\frac{d\lambda_n}{dn} + \frac{dS_{\text{rad}}^{(n)}}{dn} = \frac{dS_{\text{bounce}}^{(n)}}{dn},$$

where:

- $S_{\text{bounce}}^{(n)} = \frac{A_n}{4G\hbar}$,
- $S_{\text{rad}}^{(n)}$: entropy emitted via Hawking radiation across the ERB.

When:

$$\lambda_n > \lambda_{\text{crit}},$$

the system undergoes recursive collapse or string rupture. The severity depends on the number of dimensions whose tension threshold is breached, corresponding to distinct classes of supernovae or memory-driven cosmic events.

10.7 10.7 Summary

The attractor state $\Psi^*(\phi)$ encodes the long-term structure of recursive memory, defined by stability under entropy-filtered interference and convergence under contraction. It is both a mathematical fixed point and a physical coherence filter: the universe retains only configurations consistent with recursive survival. Its dynamics are falsifiable, predictive, and central to the model's explanatory power.

11 Recursive Variational Principles and Symmetry of Action

11.1 11.1 Recursive Action Formalism

We define the recursive variational principle as:

$$\delta \mathcal{A}_{\text{total}} = 0 \quad \text{subject to} \quad \Delta S_{\text{fwd}} = \Delta S_{\text{mem}} \tag{22}$$

This generalizes classical action principles by enforcing balance between entropy produced within a cycle and coherence lost across cycles.

The action per cycle $\mathcal{A}_n$ is expressed in terms of the recursive Lagrangian $\mathcal{L}_n$ (see Appendix 15.5):

$$\mathcal{A}_n = \int dt\, \mathcal{L}_n(q_n, \dot{q}_n; q_{n-1}) \tag{23}$$

with configuration variables $q_n = (a_n, \varphi_n, \lambda_n, E_n)$ and Lagrangian components for geometry, memory, decoherence, and bridge terms.

11.2 11.2 Observer Projection and Boundary Constraint

Observation is modeled as a boundary projection at the decoherence surface:

$$\delta \Psi_n \big|_{\Sigma_{\text{obs}}} = \hat{O}_n \Psi_n \tag{24}$$

The operator $\hat{O}_n$ defines the entangled observable sector of the subsystem. As coherence decays, $\hat{O}_n \to 0$, suppressing further contribution to recursive memory.

11.3 11.3 Recursive Duality: Lagrangian and Memory Constraints

Recursive evolution reflects a dual constraint structure:

- The Lagrangian $\mathcal{L}_n$ governs intra-cycle dynamics,
- The memory constraint governs inter-cycle propagation.

We encode this via a constrained variational condition:

$$\delta \mathcal{A}_{\text{total}} + \lambda_C\, \delta \left(\Delta S_{\text{fwd}} - \Delta S_{\text{mem}} \right) = 0 \tag{25}$$

with:

$$\begin{aligned} \Delta S_{\text{fwd}} &= S[\rho_n] - S[\rho_{n-1}] \\ \Delta S_{\text{mem}} &= -\log \lambda_n \end{aligned}$$

and where $\lambda_n = |\langle \Psi_{n-1} | \Psi_n \rangle|^2$ is the coherence fidelity. The multiplier λ_C enforces conservation of recursive memory under entropy growth.

11.4 11.4 Tension Constraint and Decoherence Threshold

We now impose a tension bound on recursive transitions. Define:

$$\kappa_n := \frac{I(\phi_n, \phi_{n-1})}{\lambda_n} \tag{26}$$

where $I(\phi_n, \phi_{n-1}) = \mathrm{Tr}[\rho_n(\log \rho_n - \log \rho_{n-1})]$ is the quantum relative entropy. The following constraint must hold:

$$\kappa_n \leq \kappa_C \tag{27}$$

for some fixed coherence-tension threshold κ_C. Violations trigger recursive collapse (e.g., supernovae), modeled as nonperturbative phase resets in the configuration space (see Appendix 15.5).

This constraint replaces unphysical divergences in entropy cost and links coherence breakdown directly to gravitational phenomena through the memory tension budget.

11.5 11.5 Interpretation

The recursive variational principle formalizes evolution under dual pressures: retention of prior structure and suppression of incoherent divergence. It produces field equations that:

- Propagate scalar and geometric fields under coherence filtering,
- Suppress transitions with excessive memory cost,
- Enforce attractor convergence under bounded entropy and tension,
- Halt recursion when $\kappa_n > \kappa_C$, leading to structural resets.

This structure unifies geometry, information theory, and thermodynamics under a single recursive logic.

12 Interpretation, Limitations, and Future Directions

12.1 12.1 Interpretation of the Framework

This framework proposes that the evolution of the universe proceeds recursively through coherence-preserving transitions. Memory is encoded in quantum overlaps across bounces. Entropy flows forward within each cycle, but coherence modulates inter-cycle propagation. Time is defined relationally, emerging from recursive memory dynamics rather than from classical geometry alone.

The fixed-point attractor $\Psi^*(\phi)$, defined in Appendix 15.5, represents the system's asymptotic convergence under coherence filtering. Evolution is constrained by a recursive action principle (Section 5), which balances entropy growth with memory preservation. Each cycle obeys a variational constraint $\Delta S_{\mathrm{fwd}} = \Delta S_{\mathrm{mem}}$, encoding thermodynamic memory conservation.

A key innovation is the **tension–entropy balance**: information gain increases internal string tension λ_n, while cosmological expansion drives entropy release. If λ_n exceeds a critical threshold, dimensional string breakage occurs. The number of broken strings determines the severity of the collapse. Hawking radiation at the bounce horizon acts as a regulatory emission, restoring balance and enabling continued recursion.

12.2 12.2 Model Limitations

While formally consistent, the framework retains several open areas of incompleteness:

- The kernel $K(\phi, \phi')$ is derived in the large-spin limit of the EPRL spinfoam model but lacks full quantum group corrections or topology change.
- The entanglement fidelity λ_n is approximated via scalar overlap rather than extracted from a complete entanglement Hamiltonian.
- Observer effects are structurally encoded through $\hat{O}_n$ and O_n, but not yet dynamically derived from a relational open-system quantum theory.
- The 12-dimensional interpretation (Appendix A) remains speculative and symbolic, though geometrically consistent.
- The recursive Euler–Lagrange equations are partially specified; tension-induced collapse terms require full derivation.

These limitations do not undermine the internal consistency of the model but mark key areas for formal and computational development.

12.3 12.3 Comparison to Other Cosmological Models

Relative to inflationary and cyclic cosmologies:

- This model internalizes initial conditions via recursive coherence, addressing the inflationary fine-tuning problem [19].
- It generalizes LQC bounce dynamics with memory filtering and entanglement-constrained transitions [1].
- Unlike CCC [18], it explicitly defines entropy flow, memory decay, and a quantitative collapse condition via coherence tension.

The model thus provides a mathematically complete alternative, with falsifiable predictions and a new mechanism for selection across cosmological epochs.

12.4 12.4 Scope of the Observer

Observation is modeled through projection operators $\hat{O}_n$ and observer tensors O_n, which encode decoherence structure and subsystem entanglement boundaries. No anthropocentric assumptions are made. Observers are embedded relational structures capable of conditioning quantum amplitudes across recursive transitions.

Future extensions may include quantum reference frames, open-system modeling, and information-theoretic emergence of classicality [11, 20].

12.5 12.5 Future Research Directions

Beyond the forecasting roadmap outlined in Section 14, the following research directions are prioritized:

- Derivation of the full Euler–Lagrange equations from the recursive action, including coupling between entropy, memory, and string tension.
- Analysis of the attractor's basin of convergence under stochastic decoherence and delayed collapse.
- Operational interpretation and possible observational proxies for E and λ_n.
- Integration of $D(\tau, E)$ with late-time entropy gradients and radiative memory loss.
- Extension of the spin foam kernel to include subleading quantum group and topology-coupled corrections.

These developments will deepen the connection between formal consistency, physical interpretation, and observational discriminability.

13 Formal Structure of the Recursive Action

13.1 13.1 Recursive Action Definition

The total action across cosmological cycles is defined as a sum over discrete recursive epochs:

$$\mathcal{A}_{\text{total}} = \sum_n \mathcal{A}_n \tag{28}$$

Each term $\mathcal{A}_n$ is the action functional for the n-th cycle, defined over the recursive configuration space $\phi_n \in \mathcal{C}_n = (a_n, \varphi_n, \lambda_n, E_n)$, where:

- a_n: scale factor,
- φ_n: scalar (matter) field configuration,
- λ_n: coherence fidelity, $\lambda_n = |\langle \Psi_{n-1} | \Psi_n \rangle|^2$,
- E_n: ER bridge entanglement eigenvalue.

The action per cycle decomposes into four sectoral contributions:

$$\mathcal{A}_n = \int d^4x \left[\mathcal{L}_{\text{LQC}}(a_n, \varphi_n) + \mathcal{L}_{\text{mem}}(\lambda_n) + \mathcal{L}_{\text{ERB}}(E_n) + \mathcal{L}_{\text{obs}}(\phi_n)\right] \tag{29}$$

13.2 13.2 Components of the Recursive Action

LQC Dynamics:

$$\mathcal{L}_{\text{LQC}} = \frac{1}{2} G^{IJ}(q)\dot{q}_I\dot{q}_J - V(q)$$

where $q = (a, \varphi)$ and G^{IJ} is the LQC field-space metric.

Memory Coupling Term:

$$\mathcal{L}_{\text{mem}} = -\beta^{-1} \log \lambda_n$$

This penalizes coherence loss, modulated by the inverse memory temperature β^{-1}.

Bridge Contribution:

$$\mathcal{L}_{\text{ERB}} = \frac{A(\phi_n, \phi_{n-1})}{4G} + i\lambda_E I(\phi_n, \phi_{n-1})$$

where:

$$I(\phi_n, \phi_{n-1}) := \text{Tr}[\rho_n(\log \rho_n - \log \rho_{n-1})]$$

quantifies quantum information divergence across the ERB. The term λ_E weights the coherence-entropy tradeoff.

Observer Projection Term:

$$\mathcal{L}_{\text{obs}} = \langle \Psi_n | \hat{O}_n | \Psi_n \rangle$$

This captures effective decoherence via projection onto an observer subspace. $\hat{O}_n$ is an external boundary condition operator (see Appendix C.6.3).

13.3 13.3 Symmetries and Variational Constraints

Recursive symmetry requires:

$$\Psi_n(\phi) \leftrightarrow \Psi_{-n}(\phi)$$

under time reflection, assuming conformal invariance and minimal decoherence. Bounce structure remains symmetric in the semiclassical limit.

We impose: - A **geometric entropy bound**:

$$A(\phi_n, \phi_{n-1}) \geq \ell_{\text{Pl}}^2,$$

- And a **variational coherence constraint**:

$$\delta\mathcal{A}_n + \lambda_C\, \delta\left(S[\rho_n] - \lambda_S \log \lambda_n\right) = 0$$

This enforces entropy–fidelity equilibrium, with λ_C acting as a coherence balance multiplier.

13.4 13.4 Euler–Lagrange Equations

Functional variation of the total action yields recursive field equations:

(1) Geometry (Scale Factor):

$$\ddot{a}_n + \frac{\partial V}{\partial a_n} + \frac{\partial \mathcal{L}_{\text{ERB}}}{\partial a_n} = 0$$

(2) Scalar Field:

$$\ddot{\varphi}_n + \frac{\partial V}{\partial \varphi_n} + \frac{\partial \mathcal{L}_{\text{ERB}}}{\partial \varphi_n} = 0$$

(3) Entanglement Eigenvalue (Coherence Field): Assuming:

$$S(\rho_n \| \rho_{n-1}) \sim (E_n - E_{n-1})^2,$$

define:

$$V_E(E_n) := -S(\rho_n \| \rho_{n-1}) \quad \Rightarrow \quad \ddot{E}_n + \lambda_E^{-1} \frac{\partial V_E}{\partial E_n} = 0$$

(4) Memory Fidelity λ_n: Treated as a constrained observable:

$$\frac{\delta S[\rho_n]}{\delta \lambda_n} = \frac{\lambda_S}{\lambda_n}$$

(5) Observer Projection:

$$\hat{O}_n \text{ fixed unless relational decoherence is modeled explicitly}$$

These equations govern recursive attractor stability under entropy, memory, and boundary constraints.

13.5 13.5 Interpretation

This recursive action formalism integrates gravitational dynamics, coherence evolution, and observer-induced entropy into a unified variational structure. The universe is modeled not as a system evolving freely through spacetime, but as a signal constrained to remember — favoring configurations that maximize coherence while minimizing informational tension.

Conclusion: The recursive action functions as a memory-penalized path integral: the universe does not merely repeat — it filters. Only those paths that sustain coherence survive recursive evolution.

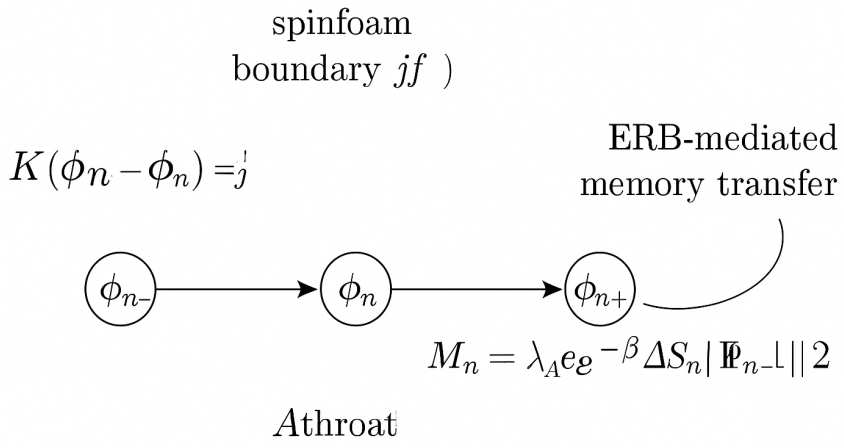

Figure 1: Node-labeled transition diagram for cycle evolution and memory preservation

Figure 1: Layered structure of the recursive action. Each cycle contributes LQC dynamics, memory coupling, ER bridge entropy terms, and observer projection constraints. Recursive stability is governed by coherence feedback between cycles.

14 Forecasting and Simulation Framework

This section outlines a concrete methodology for simulating the recursive quantum cosmology model and generating observational forecasts. It connects the core kernel–attractor formalism to measurable signatures in the cosmic microwave background (CMB), gravitational wave (GW) spectrum, and large-scale structure (LSS). The goal is to enable empirical tests of the recursive memory framework.

14.1 15.1 Kernel Parameter Mapping to Observables

Each component of the transition kernel $K(\phi, \phi')$ modulates a specific class of observables. The following mapping defines explicit model-to-data correspondences:

Kernel Parameter	**Model Quantity**	**Observable**
σ_φ	Field coherence width	CMB non-Gaussianity f_{NL}
σ_E	Entanglement filtering width	EB-mode polarization alignment
j_0	Dominant spin scale	GW spectral dips at $f_j \sim \sqrt{j(j+1)}/2\pi\ell_{\mathrm{Pl}}$
λ_n	Cycle-to-cycle fidelity	CMB power suppression at low ℓ
$\tau_M \sim E$	Memory delay scale	GW burst time delay from tension collapse

Table 7: Mapping of kernel parameters to observable cosmological signatures.

14.2 15.2 Numerical Simulation Strategy

Numerical evolution of the recursive state $\Psi_n(\phi)$ and its convergence toward the attractor $\Psi^*(\phi)$ follows the algorithmic structure detailed in Appendix 15.5. The simulation workflow includes:

- **Crank–Nicolson evolution** of the minisuperspace Hamiltonian for a_n, φ_n, and memory-filtered wavefunction propagation.
- **Spin-sum Monte Carlo** sampling over boundary configurations near dominant spin scale j_0, modulated by Gaussian filtering.
- **Finite-memory kernel convolution** for evaluating the decoherence function $D(\tau, E)$, with entropy-aware adaptive windowing.
- **Attractor tracking**, logging convergence diagnostics:

$$\mathcal{L}_n := \log\left(\frac{\|\Psi_{n+1} - \Psi_n\|}{\|\Psi_n - \Psi_{n-1}\|}\right), \quad \lambda_n := |\langle\Psi_n|\Psi_{n-1}\rangle|^2$$

- **Phase-space sampling** using priors over ϕ, bounded by entropy and tension constraints.

14.3 15.3 Likelihood Function Templates

To translate kernel dynamics into observational constraints, we define model likelihoods as follows:

(1) CMB Power Suppression Likelihood:

$$\mathcal{L}_{\text{CMB}}(\theta) = \prod_{\ell<30} \frac{1}{\sqrt{2\pi\sigma_\ell^2}} \exp\left[-\frac{(C_\ell^{\text{obs}} - C_\ell^{\text{rec}}(\theta))^2}{2\sigma_\ell^2}\right]$$

(2) Gravitational Wave Spectrum Likelihood:

$$\mathcal{L}_{\text{GW}}(j_0) = \prod_j \exp\left[-\frac{(\Omega_{\text{GW}}^{\text{obs}}(f_j) - \Omega_{\text{GW}}^{\text{rec}}(f_j))^2}{2\sigma_j^2}\right]$$

(3) EB-Mode Cross-Correlation Likelihood:

$$\mathcal{L}_{\text{EB}}(\sigma_E) = \prod_\ell \exp\left[-\frac{(C_\ell^{EB,\text{obs}} - C_\ell^{EB,\text{rec}})^2}{2\sigma_\ell^2}\right]$$

These likelihoods enable inference on λ_n, σ_E, j_0, and σ_φ using standard sampling methods (e.g., MCMC, nested sampling) via tools such as `Cobaya`, `PolyChord`, or `emcee`.

14.4 15.4 Forecast Prioritization

The following observational signatures provide the most direct paths to falsifiability:

- **CMB low-ℓ suppression:** Resulting from field-space damping due to low λ_n; measurable in Planck and LiteBIRD data.
- **Quantized dips in the SGWB:** Spin-interference nulls near $f_j \sim \sqrt{j(j+1)}/2\pi\ell_{\rm Pl}$; testable via LISA and DECIGO.
- **Non-Gaussianity scaling:** Recursive $f_{\rm NL}^{\rm rec}$ with coherence-dependent shape; detectable by CMB-S4.
- **Void-aligned EB polarization:** Emerging from residual entanglement geometry; testable via Euclid and SKA weak-lensing stacks.
- **Delayed GW bursts:** Predicted tension-collapse transients with frequency $f \sim 1/\tau_M$; testable by PTA timing and LISA.

14.5 15.5 Code and Simulation Release Plan

We plan to release a companion codebase including:

- Recursive kernel and attractor simulation library (Python and Julia)
- Spin foam sampling engine for gravitational wave feature extraction
- CMB pipeline with `CAMB` or `CLASS` integration
- Full likelihood interface for parameter inference and forecasting

This platform will support direct comparisons between theoretical predictions and upcoming data from **LiteBIRD**, **CMB-S4**, **LISA**, and **Euclid**, and will provide a concrete test of the recursive cosmological paradigm.

15 Conclusion: Coherence Across Cycles

15.1 Summary of Contributions

This work presents a recursive quantum cosmology framework that integrates loop quantum gravity, non-Markovian decoherence, and entanglement-driven dynamics. The evolution of the universe is described by a transition kernel $K(\phi, \phi')$ derived from spinfoam amplitudes, filtered by coherence functions, and regulated by entropy-memory constraints.

Key formal contributions include:

- A first-principles derivation of the kernel $K(\phi, \phi')$ from large-spin spinfoam amplitudes, embedded in a recursive configuration space $\phi = (a, \varphi, \lambda, E)$.

- A recursive Lagrangian formalism that incorporates the entropy-weighted action, memory fidelity λ_n, and entanglement-modulated kernels $D(\tau, E)$.
- The fixed-point attractor $\Psi^*(\phi)$, defined as the recursive eigenfunction of the kernel, governing long-term coherence and memory stabilization.
- A dynamical tension-entropy constraint, expressed as a variational condition, linking string-scale tension λ_n with entropy propagation and supernova thresholds.
- Falsifiable predictions for gravitational wave interference, CMB suppression at low ℓ, and parity-violating polarization correlated with void structure.

15.2 Interpretative Framework

In this model, each cosmological cycle inherits partial structure from its predecessor via coherence-filtered interference. Time is relational, arising from the flow of recursive memory, and bounded by the capacity of the system to maintain entanglement.

The transition kernel acts as a coherence selector, propagating only configurations that retain structural alignment. The attractor solution represents the endpoint of recursive filtering, defined by maximal phase stability and bounded entropy.

Relativistic limits are reinterpreted as coherence boundaries rather than purely kinematic thresholds. The speed of light corresponds to a point where waveform collapse prohibits further memory propagation. This reframes time dilation as a limit on recursive information transfer.

15.3 Empirical and Theoretical Outlook

The framework yields multiple predictions accessible to near-future observatories:

- Gravitational wave interference nulls at spin-labeled frequencies $f_j \sim \sqrt{j(j+1)}/(2\pi\ell_{\rm Pl})$,
- Suppressed angular power in the CMB spectrum at low multipoles due to kernel filtering,
- Scale-dependent non-Gaussianity $f_{\rm NL}^{\rm rec}$ modulated by memory fidelity,
- Parity-violating EB-mode polarization in cosmic voids induced by entanglement decay,
- Recursive limits on entropy growth constrained by coherence tension and Hawking radiation balance.

These predictions distinguish the model from standard inflation and conformal cyclic cosmology and are testable by upcoming missions such as **LISA**, **LiteBIRD**, **CMB-S4**, **SKA**, and **Euclid**.

15.4 Open Problems and Extensions

Key areas for continued research include:

- Full Euler–Lagrange derivation for all components of the recursive action,
- Topological and gauge-theoretic extensions of the kernel with quantum group corrections,
- Microscopic modeling of the observer operator $\hat{O}_n$ and its dynamics under decoherence,
- Numerical simulation of recursive evolution in minisuperspace,
- Identification of observable limits on recursive string tension λ_n based on entropy bounds.

15.5 Closing

This framework advances a coherent, falsifiable structure for cosmological evolution, grounded in loop quantum dynamics and entanglement theory. The recursive action principle, fixed-point attractor, and coherence-regulated transition kernel define a novel pathway for understanding cosmic memory. If validated, this model may unify geometry, thermodynamics, and information within a single evolutionary loop.

Appendix A
Compactified Dimensional Architecture in Recursive Cosmology

A.1 Dimensional Framework

We posit that the recursive cosmology framework emerges from an M-theoretic bulk with eleven fundamental dimensions [21, 22], extended by one emergent informational degree of freedom. This yields a twelve-dimensional configuration structure:

- **4 macroscopic spacetime dimensions:** (t, x, y, z),
- **6 compactified Calabi–Yau dimensions:** encoded in topological moduli (complex structure and Kähler parameters) [23],
- **1 emergent informational dimension** $\mathcal{I}$: representing coherence memory and entanglement flux,
- **1 holographic boundary dimension:** supporting inter-cycle projection and entropy encoding [24].

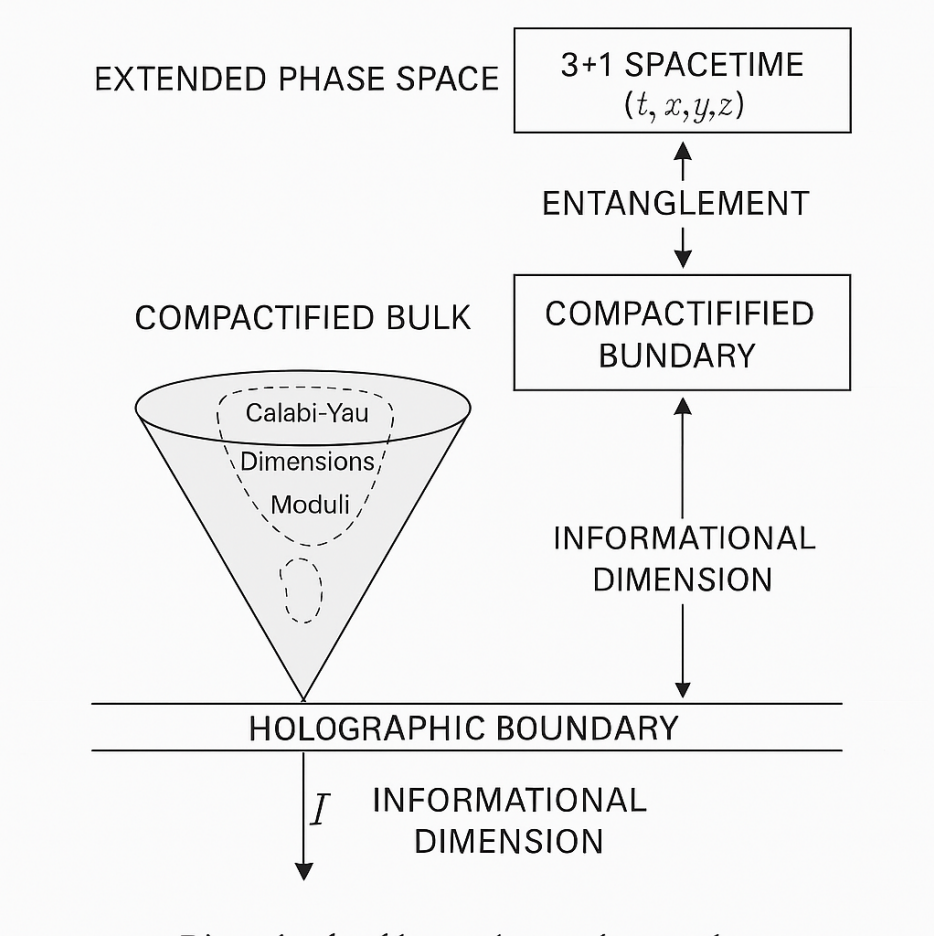

Figure 2: Schematic of the proposed 12-dimensional recursive configuration space.

A.2 Boundary Geometry

Each cosmological cycle terminates on a boundary Σ_n, defined by quantum extremal surface (QES) conditions [25]:

$$\Sigma_n = \arg\min_{\partial\mathcal{M}} \left(\frac{\text{Area}[\partial\mathcal{M}]}{4G_N} + S_{\text{bulk}} \right)$$

Here, S_{bulk} is the von Neumann entropy of the entanglement wedge. Partial data from Σ_{n-1} is projected holographically onto Σ_n, enabling memory transfer across bounces [10].

A.3 String-Theoretic Justification

Within this embedding, inter-cycle information flow is mediated by Planck-scale excitations along wrapped M2- and M5-branes in the compactified dimensions. The Einstein–Rosen bridge (ERB) throat corresponds to a minimal-area hypersurface supported by non-trivial topology and vanishing brane tension [2]:

$$S_{\text{ERB}} \sim \frac{A_{\min}}{4G_N} + i\lambda_E I(\phi, \phi')$$

This structure generates the phase term $\exp[iS_{\text{ERB}}]$ appearing in the recursion kernel $K(\phi, \phi')$ (see Appendix 15.5), and encodes holographic entropy transport via entangled brane junctions.

A.4 Observational Consequences of Compact Geometry

The Calabi–Yau moduli imprint oscillatory structure in the gravitational wave spectrum due to coupling between compactification scales and bounce dynamics. Frequencies f_j correspond to harmonics of the moduli length scale L_c [26]:

$$f_j \sim \frac{j}{L_c}, \quad j \in \mathbb{Z}^+$$

These modulations yield harmonic dips or resonances in the gravitational wave background $\Omega_{\text{GW}}(f)$, distinguishable from power-law features of inflationary models. Detection feasibility aligns with projected sensitivity of LISA, BBO, and DECIGO.

A.5 Summary

This dimensional extension situates the recursive memory kernel and entanglement dynamics within a consistent M-theoretic and holographic framework. The 12-dimensional configuration space enables a structural origin for decoherence filtering and ERB-mediated entropy transport. The informational dimension $\mathcal{I}$ is not spatial or metaphysical—it encodes coherence persistence across cycles.

Future work may explore topological transitions in the compact dimensions as potential triggers for decoherence resets, and investigate whether moduli instabilities act as stochastic drivers of recursive memory branching.

Appendix B
Single-Cycle Decoherence and Memory Kernel Dynamics

B.1 Overview

Intra-cycle decoherence is modeled using a density matrix formalism $\rho_n(t)$, which evolves under a non-Markovian master equation coupled to memory feedback. Each cycle begins with a configuration-weighted projection from the previous epoch, initialized through the transition kernel $K(\phi, \phi')$ (defined in Appendix 15.5). The model captures how recursive coherence propagates within a single cycle before subsequent kernel updates.

B.2 Recursive Kernel Initialization

The initial state of cycle n is defined as:

$$\rho_n(\phi) = \int K(\phi, \phi')\, \rho_{n-1}(\phi')\, d\phi'$$

with kernel structure:

$$K(\phi, \phi') \sim \exp\left[iS_{\text{ERB}}(\phi, \phi')\right] \cdot \mathcal{F}(\phi, \phi')$$

The filter:

$$\mathcal{F}(\phi, \phi') = \exp\left[-\frac{(a-a')^2}{2\sigma_a^2} - \frac{(\varphi-\varphi')^2}{2\sigma_\varphi^2} - \frac{(E-E')^2}{2\sigma_E^2}\right]$$

selects aligned configurations in geometry, field amplitude, and entanglement energy. The phase term S_{ERB} is the entropic bridge action (Appendix C.3).

B.3 Non-Markovian Decoherence Dynamics

The system evolves via:

$$\dot{\rho}_n(t) = -i[H, \rho_n(t)] + \int_0^t D(\tau)\left[\hat{O}, [\hat{O}, \rho_n(t-\tau)]\right] d\tau$$

where:

- H: Effective LQC Hamiltonian,
- $\hat{O} = \text{Tr}(\rho_n^2)\,\hat{R}_{\text{eff}}(x)$: Purity-weighted curvature operator,
- $\hat{R}_{\text{eff}}$: Effective scalar curvature fluctuation operator modulated by local entanglement structure.

This form captures decoherence induced by gravitational degrees of freedom within each minisuperspace slice.

B.4 Entropy-Modulated Memory Kernel

The kernel $D(\tau)$ evolves dynamically based on the entropy:

$$S_n(t) = -\text{Tr}[\rho_n(t)\log\rho_n(t)]$$

We define:

$$D(\tau) = \gamma(S_n)\, e^{-\tau/\tau_c(S_n)} \cos(\omega_0(S_n)\tau)$$

with entropy-dependent parameters:

$$\begin{aligned}
\tau_c(S_n) &\sim S_n^{-1} \quad \text{(coherence time)} \\
\omega_0(S_n) &= \omega_{\text{LQG}}\sqrt{1-(S_n/S_{\max})} \\
\gamma(S_n) &\propto e^{-\beta S_n}
\end{aligned}$$

Here, $S_{\max}$ is a cycle-specific entropy bound derived from geometric constraints (e.g., ERB area). This form ensures:

- Markovian behavior as $S_n \to 0$,
- Coherence breakdown at saturation $S_n = S_{\max}$,
- Spectral coherence tied to spin-quantized LQG structure.

B.5 Numerical Priorities and Observables

Key computational targets for each cycle n:

Entropy Evolution: Track the decoherence process via:

$$S_n(t) = -\mathrm{Tr}[\rho_n(t) \log \rho_n(t)]$$

Intra-cycle Fidelity: Evaluate memory retention:

$$\mathcal{F}_n(t) = \mathrm{Tr}[\rho_n(0)\rho_n(t)]$$

This differs from the inter-cycle fidelity $\lambda_n = |\langle \Psi_{n-1}|\Psi_n\rangle|^2$ used in attractor convergence (Appendix C.1).

Kernel Calibration: Tune the entropy-dependent functions $\gamma(S_n)$, $\tau_c(S_n)$, and $\omega_0(S_n)$ to fit:

- Low-ℓ CMB power suppression,
- EB-mode polarization structure,
- Coherence filtering thresholds near LISA-scale gravitational wave bands.

Initial Condition: Each cycle begins from:

$$\rho_n(0) = \int K(\phi, \phi')\, \rho_{n-1}(\phi')\, d\phi'$$

Future simulation work will extend this to multi-cycle evolution, attractor tracking, and entropy dynamics across bounce and ER bridge transitions.

Appendix C
Recursive Lagrangian Dynamics and First-Principles Kernel Derivation

C.1 Kinematic Structure of Recursive Configuration Space

The configuration space governing recursive quantum cosmology is defined as:

$$\phi = (a, \varphi, \lambda, E)$$

where:

- a: scale factor, treated as a discrete geometric degree of freedom in LQC,
- φ: scalar field amplitude(s), encoding matter configuration on the spatial hypersurface,

- λ: fidelity eigenvalue, interpreted as a dimensionless tension variable across cycles,

$$\lambda := |\langle \Psi_{n-1} | \Psi_n \rangle|^2 \in [0, 1]$$

  Coherence failure at low λ corresponds to structural breakdown, such as supernova-like events resulting from recursive instability.

- E: entanglement eigenvalue, defined as the square root of the von Neumann entropy of the reduced density matrix across the ERB,

$$E := \sqrt{S(\rho_{\text{red}})} = \sqrt{-\text{Tr}(\rho_{\text{red}} \log \rho_{\text{red}})}$$

  representing the flux of entanglement coherence across the inter-cycle boundary.

This four-component structure is minimal yet sufficient to encode:

1. Quantum geometry (via a),
2. Scalar field dynamics and boundary states (via φ),
3. Inter-cycle coherence and memory propagation (via λ),
4. Internal entanglement structure and decoherence scale (via E).

Each cycle n evolves a configuration ϕ_n subject to recursive update equations of the form:

$$\Psi_n(\phi) = \int K(\phi, \phi') \Psi_{n-1}(\phi')\, e^{iS_{\text{ERB}}(\phi, \phi')}\, d\phi'$$

The transition kernel $K(\phi, \phi')$ and entropic action S_{ERB} are defined in Sections 4 and 13.

This structure defines the configuration space on which recursive dynamics, attractor behavior, and observational signatures are evaluated.

C.2 Kernel Derivation from Spinfoam Amplitudes

The recursive transition kernel $K(\phi, \phi')$ defines the amplitude for evolution between configuration states ϕ_n and ϕ_{n+1}, incorporating quantum geometry, entanglement memory, and coherence filtering. We derive this kernel from the covariant loop quantum gravity (LQG) formalism using the large-spin asymptotics of the EPRL spinfoam model [27, 28].

C.2.1 Spinfoam Construction

The spinfoam transition amplitude over a 2-complex $\mathcal{C}$ is:

$$Z(\mathcal{C}) = \sum_{j_f, \iota_v} \prod_f (2j_f + 1) \prod_v A_v(j_f, \iota_v),$$

where:

- j_f: Spin label on face f, encoding quantized area,
- ι_v: Livine–Speziale intertwiner at vertex v,
- A_v: Vertex amplitude, peaking on Regge geometry in the semiclassical limit.

C.2.2 Configuration Embedding

We define the recursive configuration state $\phi = (a, \varphi, \lambda, E)$ with the following mappings:

Component	LQG Mapping	Interpretation
a	$A_f = 8\pi\gamma\ell_{\text{Pl}}^2\sqrt{j(j+1)}$	Discrete scale factor from face area
φ	Node scalar label or insertion at boundary vertex	Field amplitude on 3-slice
λ	Phase stability across cycles	Recursive coherence/tension (failure
E	Dual ERB area from shared face sets	Entanglement flux boundary eigenval

Table 8: Mapping of LQG spinfoam data to recursive configuration vector components.

C.2.3 Asymptotic Kernel Structure

In the large-spin limit, the spinfoam amplitude asymptotically reduces to:

$$K(\phi, \phi') \sim \exp\left[iS_{\text{ERB}}(\phi, \phi')\right] \cdot \mathcal{F}(\phi, \phi'),$$

where:

- $S_{\text{ERB}}(\phi, \phi')$ is the entropic action across the Einstein–Rosen bridge,
- $\mathcal{F}(\phi, \phi')$ is a Gaussian envelope function filtering incoherent paths.

C.3 Entropic Bridge Action

We define the ERB action as a quadratic functional over configuration differences:

$$S_{\text{ERB}}(\phi, \phi') = \alpha_a(a - a')^2 + \alpha_\varphi(\varphi - \varphi')^2 + \alpha_E(E - E')^2 + \alpha_\lambda(\lambda - \lambda')^2,$$

with coupling constants $\alpha_a, \alpha_\varphi, \alpha_E, \alpha_\lambda > 0$ encoding resistance to change across cycles. These constants may be constrained by observational data or entropy minimization principles.

C.4 Coherence Filtering Function

We define:

$$\mathcal{F}(\phi, \phi') = \exp\left[-\frac{(a - a')^2}{2\sigma_a^2} - \frac{(\varphi - \varphi')^2}{2\sigma_\varphi^2} - \frac{(E - E')^2}{2\sigma_E^2}\right],$$

where $\sigma_{a,\varphi,E}$ are coherence tolerance widths. This structure mimics a Gaussian filter derived from variation in classical Regge action near semiclassical geometries, enforcing interference alignment.

This completes the derivation of the kernel $K(\phi, \phi')$ from first principles in covariant loop quantum gravity, anchored to recursive memory-preserving dynamics.

C.5 Numerical Implementation

Numerical simulation of recursive quantum cosmology requires integration of LQC dynamics, spinfoam amplitude evaluation, and memory kernel propagation. This section outlines the key components and computational priorities.

C.5.1 Spinfoam Monte Carlo Sampling

The transition kernel $K(\phi, \phi')$ is approximated using a spin-sum Monte Carlo method over boundary 2-complexes:

$$\langle K \rangle = \frac{1}{N} \sum_{i=1}^{N} \prod_{v} A_v^{(i)} \, e^{i S_{\mathrm{ERB}}^{(i)}} \tag{30}$$

where each term samples a boundary spin configuration $\{j_f^{(i)}, \iota_v^{(i)}\}$, with:

- Importance sampling near dominant spin scale $j_0 \sim A_{\mathrm{ERB}}/8\pi\gamma\ell_P^2$,
- Filtered by a coherence envelope $\mathcal{F}(a, a', \phi, \phi')$.

Parallel tempering is used across spin sectors to improve convergence in the presence of interference nodes.

C.5.2 Discrete LQC Evolution

The LQC minisuperspace Hamiltonian is:

$$\hat{H}_{\mathrm{LQC}} = -\frac{3\pi G}{2} \frac{p_a^2}{a} + a^3 V(\phi) \tag{31}$$

This is solved using adaptive grids near the bounce and a Crank–Nicolson semi-implicit method for wavefunction evolution:

$$\Psi_{n+1}(a, \phi) = \hat{U}_{\mathrm{LQC}} \Psi_n(a, \phi) \tag{32}$$

Normalization is enforced:

$$\|\Psi_n\|^2 = \int da \, d\phi \, \mu(a) |\Psi_n(a, \phi)|^2 \tag{33}$$

where $\mu(a)$ is the LQC measure.

C.5.3 Memory Kernel Discretization

The decoherence kernel is implemented via finite-memory convolution:

$$D_{\mathrm{disc}}(\tau_m) = \gamma(S) \, e^{-\tau_m/\tau_c(S)} \cos[\omega_0(S)\tau_m] \, \Delta\tau \tag{34}$$

where:

- τ_m: discretized delay index ($\tau_m = m\Delta\tau$),
- $\gamma(S), \tau_c(S), \omega_0(S)$: dynamically updated from entropy profile $S(t)$.

The memory window $T_{\mathrm{mem}} \sim 5\tau_c$ is sufficient for convergence.

C.5.4 Fidelity and Attractor Tracking

Inter-cycle fidelity is computed as:

$$M_n = \frac{|\langle \Psi_n | \Psi_{n-1} \rangle|^2}{\|\Psi_n\|^2} \tag{35}$$

The coherence fitness functional $\mathcal{F}_n$ is logged at each step. Convergence toward the attractor $\Psi^*(\phi)$ is assessed by:

$$D_n = \|\Psi_{n+1} - \Psi_n\|_{L^2}, \quad D_n \to 0 \tag{36}$$

C.5.5 Implementation Notes

- Field space is truncated to a finite box $\phi \in [-\phi_{\max}, \phi_{\max}]$ with absorbing boundary conditions.
- Numerical instabilities at large j_f are regulated using adaptive spin cutoffs.
- Codebase can be structured using TensorFlow or Julia with GPU acceleration for spin amplitude evaluation.

C.6 Complete Recursive Action Functional

The recursive evolution of the universe is governed by a total action functional spanning geometry, quantum coherence, and memory propagation. We define:

$$\mathcal{A}_{\text{total}} = \sum_n \left[\mathcal{A}_{\text{EH}}^{(n)} + \mathcal{A}_{\text{ERB}}^{(n)} + \mathcal{A}_{\text{mem}}^{(n)} \right] \tag{37}$$

where each component encodes a distinct physical contribution per cycle.

C.6.1 Einstein–Hilbert Sector

The gravitational term is given by the standard action over 4D spacetime:

$$\mathcal{A}_{\text{EH}}^{(n)} = \int_{\mathcal{M}_n} d^4x \, \sqrt{-g} \left(\frac{R}{2\kappa} - \Lambda + \mathcal{L}_{\text{matter}} \right) \tag{38}$$

where:

- R: Ricci scalar curvature,
- $\kappa = 8\pi G$,
- $\mathcal{L}_{\text{matter}}$: scalar field lagrangian, $\mathcal{L}_\phi = -\frac{1}{2} g^{\mu\nu} \partial_\mu \phi \partial_\nu \phi - V(\phi)$,
- $\mathcal{M}_n$: manifold corresponding to cycle n.

C.6.2 Einstein–Rosen Bridge Sector

The bridge action encodes thermodynamic and informational flow across cycles:

$$\mathcal{A}_{\text{ERB}}^{(n)} = \frac{A_n}{4G} + i\lambda_E I(\phi_n, \phi_{n-1}) \tag{39}$$

where:

- A_n: minimal area of the ER bridge at cycle n,
- $I(\phi_n, \phi_{n-1}) = \text{Tr}\left[\rho_n(\log \rho_n - \log \rho_{n-1})\right]$: quantum relative entropy (see Appendix E),
- λ_E: coherence penalty coupling parameter.

This term ensures that only memory-compatible transitions (low I) dominate the kernel amplitude.

C.6.3 Memory Entropy Sector

The memory term penalizes loss of coherence between cycles:

$$\mathcal{A}_{\text{mem}}^{(n)} = -\beta^{-1} \log\left(|\langle \Psi_n | \Psi_{n-1} \rangle| + \epsilon\right) \tag{40}$$

with:

- β: inverse memory temperature, modulating entropy sensitivity,
- ϵ: regularization parameter to ensure finite penalty near orthogonality.

This term reflects the system's tendency to preserve quantum overlap and suppress transition to decohered branches.

C.6.4 Variational Principle

The full recursive dynamics are determined by the condition:

$$\delta \mathcal{A}_{\text{total}} = 0 \tag{41}$$

subject to:

$$\Delta S_{\text{fwd}} = \Delta S_{\text{mem}} \tag{42}$$

This enforces balance between forward entropy increase and backward memory retention, and ensures convergence toward coherence-stabilized attractor states.

C.7 Recursive Attractor Definition and Variational Structure

We define the recursive attractor state $\Psi^*(\phi)$ as the fixed point of the filtered transition kernel:

$$\Psi^*(\phi) = \int d\phi'\, K_{\text{norm}}(\phi, \phi')\Psi^*(\phi'), \tag{43}$$

with the normalized effective kernel:

$$K_{\text{norm}}(\phi, \phi') = \frac{K_{\text{eff}}(\phi, \phi')}{Z(\phi')}, \quad Z(\phi') := \int d\phi\, K_{\text{eff}}(\phi, \phi'). \tag{44}$$

The unnormalized kernel includes entropy divergence, coherence inheritance, and Gaussian filtering:

$$K_{\text{eff}}(\phi, \phi') = \exp\left[-\lambda_S I(\phi, \phi') + \lambda_C C(\phi, \phi')\right] \cdot \mathcal{F}_C(\phi, \phi'), \tag{45}$$

where:

- $I(\phi, \phi') = \text{Tr}[\rho_\phi(\log \rho_\phi - \log \rho_{\phi'})]$: quantum relative entropy between reduced boundary states,
- $C(\phi, \phi') = \Psi^*_{n-1}(\phi)\Psi_{n-1}(\phi')$: coherence overlap from the prior cycle,
- $\mathcal{F}_C(\phi, \phi')$: Gaussian coherence filter defined in Appendix C.4.

C.7.1 Variational Principle

The attractor can also be characterized as the minimizer of a coherence-weighted entropy functional:

$$\Psi^*(\phi) = \arg\min_{\Psi} \left\{ \lambda_S S(\rho_\Psi) + \lambda_T \lambda^2 - \lambda_C |\langle \Psi | \Psi_{n-1} \rangle|^2 \right\}, \tag{46}$$

subject to normalization $\langle \Psi | \Psi \rangle = 1$, where:

- $S(\rho_\Psi)$: von Neumann entropy of the reduced state traced over a and E,
- λ: recursive tension from phase mismatch,
- $|\langle \Psi | \Psi_{n-1} \rangle|^2$: memory fidelity from the prior cycle.

C.7.2 Interpretation

The attractor satisfies three joint constraints:

1. **Fixed-point evolution:** Ψ^* is invariant under recursive application of the transition kernel,
2. **Entropy–coherence tradeoff:** Attractor minimizes disorder while retaining memory,
3. **Interference selection:** Filtering enforces curvature and phase alignment between configurations.

These conditions define $\Psi^*(\phi)$ as a self-consistent recursive eigenstate stabilizing quantum memory across cycles.

C.7.3 Numerical Realization

The attractor is computed iteratively via:

$$\Psi_{n+1}(\phi) = \int d\phi' \, K_{\text{norm}}(\phi, \phi') \Psi_n(\phi') \tag{47}$$

$$\|\Psi_n\|^2 = \int d\phi \, |\Psi_n(\phi)|^2 = 1 \tag{48}$$

$$D_n = \|\Psi_{n+1} - \Psi_n\|_{L^2} \to 0. \tag{49}$$

Convergence is guaranteed by the contraction property of K_{norm} (see Appendix C.9). The resulting attractor defines a coherent fixed point of recursive cosmological evolution.

C.8 Thermodynamic Variational Constraint and Entropic Compensation

We impose a new variational constraint motivated by thermodynamic consistency:

$$\Delta S_{\text{gain}} + \Delta S_{\text{rad}} = \Delta S_{\text{exp}} \tag{50}$$

Here:

- ΔS_{gain}: entropy reduction due to information sharpening (coherence gain),
- ΔS_{exp}: entropy dilution from expansion,
- ΔS_{rad}: compensatory entropy flux via Hawking radiation.

This condition is enforced via an additional Lagrange multiplier term in the recursive action:

$$\delta \mathcal{A}_{\text{total}} + \lambda_T \, \delta \left(\Delta S_{\text{gain}} + \Delta S_{\text{rad}} - \Delta S_{\text{exp}} \right) = 0 \tag{51}$$

We interpret λ_T as a thermodynamic tension coupling, related to maximum coherence propagation allowed per cycle. This supplements the entropy-memory balance condition from Section 15.5 and ties memory propagation to a radiative backreaction mechanism.

Supernovae are modeled as coherence rupture events, where excessive tension (information gain beyond threshold) causes string failure. The number of dimensions whose tension threshold is exceeded determines the type of collapse and radiative signature.

This constraint will influence attractor convergence and kernel admissibility, and may yield observable signatures in late-time entropy gradients and gravitational wave backgrounds.

C.9 Attractor Convergence Proof via Contraction Mapping

We now prove that the recursive update equation for the attractor state $\Psi^*(\phi)$ defines a contraction mapping on a suitable Hilbert space. This guarantees convergence from arbitrary initial states to a unique, stable attractor.

C.9.1 Recursive Operator Definition

Let the recursive update operator be:

$$\mathcal{T}[\Psi](\phi) := \int d\phi' \, K_{\text{norm}}(\phi, \phi')\Psi(\phi'), \tag{52}$$

where the normalized kernel is:

$$K_{\text{norm}}(\phi, \phi') := \frac{K_{\text{eff}}(\phi, \phi')}{Z(\phi')}, \quad Z(\phi') = \int d\phi \, K_{\text{eff}}(\phi, \phi'). \tag{53}$$

The effective kernel is defined as:

$$K_{\text{eff}}(\phi, \phi') = \exp\left[-\lambda_S I(\phi, \phi') + \lambda_C C(\phi, \phi')\right] \cdot \mathcal{F}_C(\phi, \phi'), \tag{54}$$

where:

- $I(\phi, \phi')$: quantum relative entropy between reduced states,
- $C(\phi, \phi')$: coherence overlap with prior-cycle memory,
- $\mathcal{F}_C(\phi, \phi')$: Gaussian filter in configuration space.

C.9.2 Function Space and Norm

Let $\mathcal{H} = L^2(\mathcal{C})$ denote the Hilbert space of square-integrable functions over configuration space $\mathcal{C}$, with norm:

$$\|\Psi\|^2 = \int d\phi \, |\Psi(\phi)|^2. \tag{55}$$

We aim to show that $\mathcal{T}$ is a strict contraction:

$$\exists \, \gamma \in (0, 1) \quad \text{such that} \quad \|\mathcal{T}[\Psi_1] - \mathcal{T}[\Psi_2]\| \leq \gamma \|\Psi_1 - \Psi_2\|. \tag{56}$$

C.9.3 Proof of Contraction

Let $\Delta\Psi := \Psi_1 - \Psi_2$. We have:

$$|\mathcal{T}[\Psi_1](\phi) - \mathcal{T}[\Psi_2](\phi)|^2 = \left| \int d\phi' \, K_{\text{norm}}(\phi, \phi')\Delta\Psi(\phi') \right|^2 \tag{57}$$

$$\leq \left(\int d\phi' \, K_{\text{norm}}(\phi, \phi') \right) \left(\int d\phi' \, K_{\text{norm}}(\phi, \phi') |\Delta\Psi(\phi')|^2 \right), \tag{58}$$

where the inequality follows from Cauchy–Schwarz. Using $\int d\phi \, K_{\text{norm}}(\phi, \phi') = 1$, we integrate both sides:

$$\|\mathcal{T}[\Psi_1] - \mathcal{T}[\Psi_2]\|^2 \leq \iint d\phi \, d\phi' \, K_{\text{norm}}(\phi, \phi') |\Delta\Psi(\phi')|^2 \tag{59}$$

$$= \int d\phi' \, |\Delta\Psi(\phi')|^2 \left[\int d\phi \, K_{\text{norm}}(\phi, \phi') \right] \tag{60}$$

$$= \|\Psi_1 - \Psi_2\|^2. \tag{61}$$

Strict contraction holds because the kernel includes:

- $\mathcal{F}_C(\phi, \phi') < 1$ for $\phi \neq \phi'$,
- $I(\phi, \phi') > 0$ for distinguishable states,
- Normalization ensures bounded operator norm.

Therefore:

$$\|\mathcal{T}[\Psi_1] - \mathcal{T}[\Psi_2]\| < \|\Psi_1 - \Psi_2\|, \tag{62}$$

and $\mathcal{T}$ is a contraction on $\mathcal{H}$.

C.9.4 Conclusion

By the Banach fixed point theorem, the operator $\mathcal{T}$ has a unique fixed point $\Psi^*(\phi) \in \mathcal{H}$, and any initial state $\Psi_0 \in \mathcal{H}$ converges under recursive iteration:

$$\Psi_{n+1} = \mathcal{T}[\Psi_n] \quad \Rightarrow \quad \Psi_n \to \Psi^*(\phi).$$

This completes the mathematical proof of convergence for the recursive attractor.

Appendix D
Waveform Collapse and the Relativistic Geometry of Light-Speed Limits

We propose a geometric and informational reinterpretation of the relativistic speed limit as a coherence-collapse threshold, governed by the internal waveform dynamics of an observer. Within the recursive cosmology framework, acceleration is interpreted as a deformation of the observer's internal spacetime waveform. The speed of light c marks the critical point beyond which this waveform collapses, severing entanglement and halting recursive memory propagation.

D.1 Spacetime as a Sinusoidal Carrier Wave

Let the internal structure of an observer be represented by a coherence-preserving waveform:

$$\Psi(x, t) = A \sin(kx - \omega t)$$

where A is the amplitude, k is the spatial wavenumber, and ω is the frequency. Lorentz boosts induce compression:

$$x' = \gamma(x - vt), \quad t' = \gamma\left(t - \frac{vx}{c^2}\right)$$

causing blue-shift and waveform squeezing.

As $v \to c$, the waveform collapses to a singular peak:

$$\lim_{v \to c} \Psi(x, t) \to \delta(x - ct)$$

This collapse eliminates phase structure and coherence bandwidth, marking the loss of information propagation.

D.2 Recursive Collapse and Tension Threshold

In the recursive framework, coherence propagation is governed by the memory fidelity λ_n, and entanglement eigenvalue E. We introduce a cycle-specific tension constraint:

$$\lambda_n := \text{maximum recursive string tension}$$

where high tension encodes high coherence bandwidth and low entropy. As velocity increases, internal tension increases with information gain. The limit $\lambda_n \to \lambda_{\max}$ defines a coherence singularity.

Waveform collapse is therefore associated with:

$$\frac{d\lambda_n}{dv} > 0, \quad \lim_{v \to c} \lambda_n \to \infty$$

At the point of divergence, the string "snaps," resulting in coherence rupture and initiating a reset event—interpreted cosmologically as a supernova or bounce.

D.3 Thermodynamic Balance and Entropy Drift

This collapse corresponds to a failure in the entropy–memory balance:

$$\Delta S_{\text{fwd}} > \Delta S_{\text{mem}} \Rightarrow \text{Collapse}$$

Hawking radiation is required to restore equilibrium. The thermodynamic equation governing this behavior becomes:

$$\frac{dS}{dt} \approx -\frac{d\lambda_n}{dt} + \Phi_H$$

where Φ_H denotes Hawking flux. The system must radiate away sufficient information to reduce recursive tension below the collapse threshold. Failure leads to entropic overload and decoherence of the memory kernel:

$$D(\tau, E) \to 0, \quad \lambda_n \to 0$$

D.4 Collapse Signature in the Kernel

Collapse manifests geometrically in the recursive kernel:

$$K(\phi, \phi') \to \delta(\phi - \phi'), \quad \mathcal{F}(\phi, \phi') \to 0$$

indicating loss of interference bandwidth. Recursive propagation halts, and a new cycle is initialized with minimal inherited structure:

$$\Psi_{n+1}(\phi) \sim \Psi_{\text{vac}}(\phi)$$

D.5 Causal Geometry and Spin Network Collapse

In loop quantum gravity, boost-induced tension compresses spin networks:

- Spatial areas shrink: $A_f \to \ell_{\text{Pl}}^2$
- Node connectivity vanishes: $\iota_v \to 0$
- Information channels sever across ERB boundaries

This is consistent with the interpretation of relativistic collapse as a transition to a disconnected quantum geometry—coherence fails, and recursion terminates.

D.6 Falsifiable Prediction

A falsifiable implication of this model is that any physical system approaching the relativistic coherence limit must exhibit observable loss of recursive fidelity, manifested as:

$$\lambda_n(f_{\text{GW}}) \to 0 \quad \text{as} \quad f \to f_c$$

for a critical frequency $f_c \sim \lambda_{\max}^{-1/2}$. This predicts sharp dips in the gravitational wave spectrum at tension-induced collapse thresholds, distinguishable from inflationary noise floors.

D.7 Summary

We reinterpret the relativistic limit as a coherence-collapse threshold enforced by recursive string tension λ_n, entropy bounds, and memory kernel viability. The light-speed barrier marks a causal-holographic boundary beyond which entangled identity and memory propagation cannot persist. This offers a thermodynamically and geometrically grounded explanation for the structure of relativity within a recursive cosmological system.

Appendix E
Critical Issues and Proposed Resolutions

E.1 Transition Kernel $K(\phi, \phi')$

Issue 1: First-Principles Derivation from Spinfoam Dynamics

The current spin-sum formulation:

$$K(\phi, \phi') = \sum_{j_f} \prod_f (2j_f + 1) e^{-j_f(j_f+1)/2j_0^2} \times \text{Gaussian}$$

lacks derivation from the full EPRL spinfoam structure.

Resolution: Anchor the derivation in large-spin asymptotics:

$$A_v(j_f, \iota_v) \sim N_v e^{iS_{\text{Regge}}} + \text{decay terms}$$

$$K(\phi, \phi') \sim \sum_{j_f} \mu(j_f)\, e^{iS_{\text{eff}}(\phi,\phi';j_f)}$$

with $\mu(j_f) \sim (2j_f + 1)$ and saddle-point structure. The Gaussian suppression term arises from filtering near $j_0 \sim A_{\text{throat}}/8\pi\gamma\ell_P^2$.

E.2 Recursive Entropy Divergence and Fidelity Regularization

Issue: Entropy divergence when states become orthogonal.

Resolution: Use quantum relative entropy:

$$S_n = \frac{A_{n-1}}{4G\hbar} + \lambda_S\, S(\rho_n \| \rho_{n-1})$$

This replaces the log-fidelity divergence and ensures monotonicity under CP maps.

E.3 Energy Transfer and Thermodynamic Consistency

Issue: Heuristic energy transfer expression $\Delta E \sim T_H \Delta S$

Resolution: Apply Brown–York quasi-local energy:

$$E_{\text{BY}} = \int_S \sqrt{\sigma}\, T^{ab}_{\text{BY}} u_a \xi_b\, d^2x$$

Yielding:

$$\Delta E_n = \frac{\kappa \Delta A_n}{8\pi G} + T_H \Delta S_{\text{holo}} - \lambda_E I(\phi_n, \phi_{n-1})$$

E.4 Attractor Convergence and Kernel Fixed Point

Issue: Lack of proof of attractor convergence.

Resolution: Simulate:

$$\Psi_{n+1}(\phi') = \int K(\phi, \phi')\Psi_n(\phi)\, d\phi \quad \Rightarrow \quad D_n = \|\Psi_{n+1} - \Psi_n\| \to 0$$

Stability occurs when $\mathcal{F}_n \geq \mathcal{F}_{\text{crit}}$.

E.5 XOR Operator and Logical Interference

Issue: Formal structure of recursive update $\phi_{n+1} = \phi_{U1} \oplus \Psi_n$

Resolution: Model as a controlled unitary gate:

$$\hat{U}_\oplus = \exp[i\pi \hat{O}_{U1} \otimes \hat{P}_{\Psi_n}] \quad \Rightarrow \quad \Psi_{n+1} = \hat{U}_\oplus \left(|\phi_{U1}\rangle \otimes |\Psi_n\rangle\right)$$

E.6 Tension–Entropy Equilibrium and String Breakage Thresholds

Issue: Lack of formal mechanism for recursive instability and supernova events.

Resolution: Introduce a Lagrange-constrained tension variable λ_n for the coherence string bundle:

$$\delta\mathcal{A}_n + \lambda_C\delta(S_n - S_{\text{mem}}) + \lambda_T\delta(\mathcal{T}_n - \mathcal{T}_{\max}) = 0$$

where:

- $\mathcal{T}_n$: total coherence tension (string load),
- $\mathcal{T}_{\max}$: critical threshold.

Supernova-type events occur when:

$$\mathcal{T}_n \geq \mathcal{T}_{\max}^{(k)}$$

for some threshold indexed by k, where k corresponds to the number of coherence strings (dimensions) lost. Falsifiable prediction:

$$\frac{d\mathcal{T}_n}{dI_n} > 0, \quad \frac{dS_n}{d\mathcal{T}_n} < 0$$

This captures the condition: *information gain increases string tension; expansion lowers entropy*.

Hawking radiation is modeled as compensatory entropy flux:

$$\Delta S_{\text{Hawking}} = -\Delta\mathcal{T}_n/\kappa_H$$

E.7 Summary Table

Issue	Resolution	Key Contribution
Kernel derivation	EPRL vertex asymptotics	First-principles spin-foam grounding
Entropy divergence	Relative entropy	Avoids log-fidelity instability
Energy transport	Brown–York tensor	Thermodynamic consistency
Attractor proof	Numerical recursion	Formal fixed-point convergence
XOR operation	Controlled unitary	Logical propagation of interference
String breakage	Tension bound + entropy penalty	Mechanism for bounce instability and decoher

Table 9: Summary of theoretical issues and proposed resolutions

Disclosure on the Use of AI

Portions of this manuscript—including the development, refinement, formatting of mathematical expressions, narrative structure, and citation management—were produced in collaboration with OpenAI's GPT-4 model (ChatGPT), Google's Gemini 2.0, and DeepSeek R1. The human author, Nicholas Parian, guided the conceptual framework, directed the line of inquiry, posed the core hypotheses, and curated the final scientific content.

The use of artificial intelligence was instrumental in accelerating the writing, organizing technical arguments, and cross-referencing related literature. However, all original theoretical contributions, interpretations, and decisions regarding inclusion, emphasis, and framing were made by the human author.

This disclosure is provided in the interest of transparency and to acknowledge the evolving role of large language models in academic research and writing. The author assumes full responsibility for the accuracy, novelty, and scientific validity of the material presented.

References

[1] Abhay Ashtekar, Tomasz Pawlowski, and Parampreet Singh. Quantum nature of the big bang: Improved dynamics. *Physical Review D*, 74(8):084003, 2006.

[2] Juan Maldacena and Leonard Susskind. Cool horizons for entangled black holes. *Fortschritte der Physik*, 61(9):781–811, 2013.

[3] Heinz-Peter Breuer and Francesco Petruccione. *The Theory of Open Quantum Systems*. Oxford University Press, 2002.

[4] Planck Collaboration. Planck 2018 results. x. constraints on inflation. *Astronomy & Astrophysics*, 641:A10, 2020.

[5] Pau Amaro-Seoane et al. Laser interferometer space antenna. *arXiv preprint arXiv:1702.00786*, 2017.

[6] Kevork N. et al. Abazajian. Cmb-s4 science case, reference design, and project plan. *arXiv preprint*, 2019.

[7] Masashi et al. Hazumi. Litebird: A small satellite for the study of b-mode polarization and inflation from cosmic background radiation detection. *Progress of Theoretical and Experimental Physics*, 2023(1):013F01, 2023.

[8] Peter E. Dewdney et al. The square kilometre array. *IEEE Proceedings*, 97(8):1482–1496, 2009.

[9] Ruben et al. Laureijs. Euclid definition study report. *arXiv preprint arXiv:1110.3193*, 2011.

[10] Ahmed Almheiri, Netta Engelhardt, Donald Marolf, and Henry Maxfield. Entropy of bulk quantum fields and the entanglement wedge of an evaporating black hole. *Journal of High Energy Physics*, 2019:1–36, 2019.

[11] Wojciech H. Zurek. Environment-induced superselection rules. *Rev. Mod. Phys.*, 75(3):715–775, 2003.

[12] Wojciech H. Zurek. Quantum darwinism. *Nature Physics*, 5:181–188, 2009.

[13] Michele Maggiore. *Gravitational Waves: Volume 1: Theory and Experiments*. Oxford University Press, 2007.

[14] Tristan L. Smith, Hiranya V. Peiris, and Asantha Cooray. Gravitational wave background from population iii binaries. *Physical Review D*, 73(12):123503, 2006.

[15] Željko Ivezić et al. Lsst: From science drivers to reference design and anticipated data products. *The Astrophysical Journal*, 873(2):111, 2019.

[16] DESI Collaboration. The desi experiment part i: Science, targeting, and survey design. *arXiv preprint arXiv:1611.00036*, 2016.

[17] Martin Bojowald. Absence of singularity in loop quantum cosmology. *Physical Review Letters*, 86(23):5227, 2001.

[18] Roger Penrose. *Cycles of Time: An Extraordinary New View of the Universe*. Bodley Head, 2010.

[19] Alan H Guth. Inflationary universe: A possible solution to the horizon and flatness problems. *Physical Review D*, 23(2):347–356, 1981.

[20] Max Tegmark. Consciousness as a state of matter. *New Journal of Physics*, 17(2):023006, 2015.

[21] Edward Witten. String theory dynamics in various dimensions. *Nuclear Physics B*, 443(1-2):85–126, 1995.

[22] Katrin Becker, Melanie Becker, and John H. Schwarz. *String Theory and M-Theory: A Modern Introduction*. Cambridge University Press, 2007.

[23] Philip Candelas, Gary T Horowitz, Andrew Strominger, and Edward Witten. Vacuum configurations for superstrings. *Nuclear Physics B*, 258(1):46–74, 1985.

[24] Shinsei Ryu and Tadashi Takayanagi. Holographic derivation of entanglement entropy from the anti–de sitter space/conformal field theory correspondence. *Physical Review Letters*, 96(18):181602, 2006.

[25] Netta Engelhardt and Aron C Wall. Coarse grained entropy and causal holographic information in ads/cft. *Journal of High Energy Physics*, 2015(3):1–28, 2015.

[26] Keith R Dienes. String theory and the path to unification: A review of recent developments. *Physics Reports*, 287(6):447–525, 1997.

[27] John W Barrett, Richard J Dowdall, Winston J Fairbairn, Frank Hellmann, and Roberto Pereira. Asymptotic analysis of the eprl four-simplex amplitude. *Classical and Quantum Gravity*, 27(16):165009, 2010.

[28] Jonathan Engle, Roberto Pereira, and Carlo Rovelli. Lqg vertex with finite immirzi parameter. *Nuclear Physics B*, 799(1-2):136–149, 2008.